学　位　論　文

Doctor's Thesis

Analyses of α/β Hydrolase Domain Containing 2 Mutant Mice Established by Gene Trap

（遺伝子トラップ法により樹立した
α/β Hydrolase Domain Containing 2 変異マウスの解析　）

宮　田　　敬　士

Keishi　Miyata

熊本大学大学院医学研究科博士課程内科系専攻循環器内科学

指導：　小川　　久雄　教授

指導：大久保　博晶　教授

２００５年度

学 位 論 文

Doctor's Thesis

論文題名 : Analyses of α/β Hydrolase Domain Containing 2 Mutant Mice Established by Gene Trap

（ 遺伝子トラップ法により樹立した α/β Hydrolase Domain Containing 2 変異マウスの解析 ）

著 者 名： 宮 田 敬 士

Keishi Miyata

指導教官名：	循環器病態学担当教授	小 川 久 雄
	神経発生分野担当教授	大久保 博 晶
審査委員名：	代謝内科学担当教授	荒 木 栄 一
	細胞病理学担当教授	竹 屋 元 裕
	生体機能薬理学担当教授	光 山 勝 慶
	腫瘍医学担当教授	佐 谷 秀 行

２００５年度

Contents

Summary

In the development of atherosclerosis, multiple stages including the migration of vascular smooth muscle cells (SMCs) are involved. To search for genes which are involved in these stages, we screened mutant mouse lines established by the exchangeable gene trap method utilizing X-gal staining during their embryonic development. One of these lines, Ayu8025, showed abundant reporter gene expression in the vitelline vessels of yolk sacs at embryonic day (E) 12.5. The trap vector was inserted into the 5th intron of α/β hydrolase domain containing 2 (*Abhd2*) gene which was shown to be expressed in vascular and non-vascular SMCs of adult mice. Although Abhd2$^{Gt/Gt}$ homozygous mice were apparently normal, enhanced SMC migration in the explants SMCs culture and marked intimal hyperplasia after cuff placement were observed in Abhd2$^{Gt/Gt}$ homozygous mice in comparison with wild-type mice. These results suggest *Abhd2* has an apparent anti-atherosclerosis effect on vascular SMCs.

Publication List

Keishi Miyata [1,2], Yuichi Oike[3], Takayuki Hoshii[1], Hiromitsu Maekawa[3], Hisao Ogawa[2], Toshio Suda[3], Kimi Araki[1] and Ken-ichi Yamamura[1]

" Increase of smooth muscle cell migration and of intimal hyperplasia in mice lacking the α/β hydrolase domain containing 2 gene. "

Biochemical and Biophysical Research Communication. *2005 Apr 1:329(1):296-304*

[1]Department of Developmental Genetics, Institute of Molecular Embryology and Genetics, Kumamoto University, 4-24-1 Kuhonji, Kumamoto 862-0976, Japan.

[2]Department of Cardiovascular Medicine, Graduate School of Medical Sciences, Kumamoto University, 1-1-1 Honjo, Kumamoto 860-8556, Japan.

[3]Department of Cell Differentiation, The Sakaguchi Laboratory, Keio University School of Medicine, Tokyo 160-8582, Japan.

Acknowledgements

These series of investigations took place during my four years of graduate study in the Department of Cell Differentiation (2000.4-2002.3) and the Department of Development of Genetics (2002.4-2004.3), Institute of Molecular Embryology and Genetics (IMEG), Kumamoto University.

I am grateful to great supports by Professor Ken-ichi Yamamura, Department of Developmental Genetics, IMEG, Kumamoto University, Professor Suda Toshio, Department of Cell Differentiation, The Sakaguchi Laboratory, Keio University School of Medicine (the former Professor in the Department of Cell Differentiation, IMEG, Kumamoto University) and Professor Hisao Ogawa, Department of Cardiovascular Medicine, Kumamoto University. I gratefully acknowledge the advice and encouragement from Dr. Yuichi Oike, Department of Cell Differentiation, The Sakaguchi Laboratory, Keio University School of Medicine, and Associate Professor Kimi Araki, Department of Developmental Genetics, IMEG, Kumamoto University. I learned a lot about biological science from them. Studies done in this laboratory were very worthwhile experience for me. I am also grateful to Ms. Nakata for technical assistance such as immuno-histochemical work and all colleagues, of past and present, Department of Developmental Genetics, IMEG, Kumamoto University.

Finally, I would like to delicate this work to my family for their supports and tolerances, and especially to my son Shuto and my wife Emi who encouraged me and supported my scientific career.

Abbreviation

Abhd: α/β hydrolase domain containing

Asp: Aspartic acid

bFGF: basic fibroblast growth factor

BM: Bone marrow

BrdU: Bromodeoxyurine

BSA: Bovine serum albumin

Cys: Cysteine

DIG: Digoxigenin

DMEM: Dulbecco's modified Eagle's medium

EB: Embryoid body

ES: Embryonic stem

FCS: Fetal bovine serum

Glu: Glutamic acid

His: Histidine

HRP: Horseradish peroxidase

IRES: Internal ribosome entry site

LABH: Lung α/β hydrolase

2-ME: 2-Mercaptoethanol

PBS: Phosphate-buffer saline

PCR: Polymerase chain reaction

PDGF: Platelet-derived growth factor

RACE: Rapid amplification of cDNA ends

RT: Room temperature

RT-PCR: Reverse-transcription polymerase chain reaction

SDS: Sodium dodecyl sulfate

Ser: Serine

SMA: Smooth muscle actin

SMC: Smooth muscle cell

TGFβ : Transforming growth factor β

Introduction

Smooth muscle cells (SMCs) of the vascular system form an intriguing population of cells that are relevant for maintaining vascular tone and function. Many vasoactive factors for SMCs, including platelet-derived growth factor-BB (PDGF-BB), basic fibroblast growth factor (bFGF), epidermal growth factor (EGF), transforming growth factor beta-1 (TGF-β1) and tumor necrosis factor α (TNFα) are known to regulate regional proliferation and migration of SMCs, and involved in the pathogenesis of atherosclerosis.

Atherosclerosis is characterized by smooth muscle cell hyperplasia or hypertrophy and matrix protein accumulation in the intima and/or media with or without lipid deposition, resulting in thickening and stiffness of arterial wall (Stary et al. 1994) (Fig.1). Atherosclerosis includes spontaneous atherosclerosis, accelerated atherosclerosis (namely, transplant atherosclerosis), vein-graft atherosclerosis, and angioplasty-induced restenosis (Ip et al. 1990). The use of animal models in the study of atherosclerosis is essential to answer many questions. Recent advances in embryo manipulation techniques have produced various genetically modified mice to analyze the role of specific molecules in the pathogenesis and therapy of atherosclerosis. Many mouse models, such as hypercholesterolemia-induced atherosclerosis (Plump et al. 1992), transplant-induced atherosclerosis (Nagano et al. 1997) and angiogenesis (Couffinhal et al. 1998), have been established. Angioplasty

is very often used to treat patients with coronary artery disease. The coronary blood flow in the majority of patients is recovered after treatment. The problem is restenosis of vessel because of the formation of neointimal lesions (Levine et al. 1995). The hallmarks of neointima lesions are SMC proliferation and extracellular matrix deposition (Schwartz et al. 1995). The pathogenesis of this disease remains poorly understood. Most knowledge concerning the mechanisms of restenosis formation was derived from studies of animal models. In the late 1970s, Clowes et al. established the rat arterial injury model (Clowes et al. 1977). In 1993, Lindner et al. developed the first mouse model of arterial injury using a flexible wire (Lindner et al. 1993). Subsequently, ligation and cuff injury models were established. Using these models, many articles describing the process of restenosis were published.

Recently, smooth muscle-associated protein 8 (smap8), epoxide hydrolase and retinoid-inducible serine carboxypeptidase (RISC), which are members of the α/β hydrolase family, are reported to associate with the vascular smooth muscle cell and the progression of atherosclerosis (Chen et al. 2001; Davis et al. 2002; Nishimoto et al. 2003). And also, Fornage et al. have reported that epoxide hydrolase, one of these family members, plays an important role in the pathogenesis of atherosclerosis in human by a polymorphism study (Fornage et al. 2004).

The α/β hydrolase fold family is a large variety of hydrolytic enzymes of widely differing phylogenetic origin. Each of these family members has the same protein fold, termed as the α/β hydrolase fold (Ollis et al. 1992; Holmquist 2000).

The differences between the functions of these hydrolytic enzymes reside in their substrate specificity. All of these proteins share a common fold formed by an α/β sheet of five to eight β-sheets connected by α-helices to form an α/β/α sandwich (Fig. 2). In most of the family members, the β-strands are parallel; some though show an inversion in the order of the first strands, resulting in an antiparallel orientation. These enzymes diverge from a common ancestor so they preserve the arrangement of the catalytic residues, not the binding sites. The active site of all these enzymes is always located in the same position in the structure. There are usually three key residues responsible for the catalytic activity in the active site: nucleophile, histidine, and acid, which are classically known as the catalytic triad (Schrag and Cygler 1997). The nucleophile can be a Ser, Cys or Asp residue while the acid loops accommodate an Asp or Glu residue. The three residues are close in structure, but do not form a local sequence motif because they are distant in protein sequence. The functional roles of the triad residues are as fellow: the sidechain group at nucleophile serves as nucleophilic center, histidine sidechain acts as a general base and is hydrogen bonded to the carboxylic group of the acid sidechain. Histidine and acid residues together form a charge relay system.

During evolution structural similarity is preserved much longer than sequence similarity. Although the ESTHER database (http://bioweb.ensam.inra.fr/esther) presents information on all α/β hydrolase fold proteins, it focuses on a smaller group of proteins of the superfamily for which

sequence homology can be detected. This group of sequences includes cholinesterases/carboxylesterases group (acetylcholinesterase, cholesterol esterase, cholinesterase and carboxylesterase) (C-Block), lipase group (hepatic lipase, pancreatic lipase, and phospholipase) (L-Block), hormone sensitive lipases (H-Block) and all other protein (epoxide hydrolase, haloperoxidase, thioesterase and thioesterase)(X-Block) (Fig. 3).

Recently, Edgar et al. reported that three novel mouse cDNA encoding proteins containing an α/β hydrolase fold were cloned from lung cDNA (Edgar and Polak 2002); their cDNAs were named as lung α/β hydrolase (Labh) 1, 2 and 3. These are now termed as α/β hydrolase domain containing (Abhd) 1, 2 or 3. These three mouse Abhd proteins are members of conserved protein family which are found in all species examined (Fig. 4). RT-PCR analyses showed that these three genes are widely, but differentially expressed in many tissues. The expression of *Abhd1* and *Abhd3* was highest in the liver and lowest in the spleen, whereas the expression of *Abhd2* was high in the testis and the spleen. The *Abhd1* catalytic triad was identified as Ser211, Asp337, and His366. In addition, all three Abhd proteins are shown to have a single predicted amino-terminus trans-membrane domain. Although proteins in this family generally act as enzymes such as dienelactone hydrolases, haloalkane dehalogenases, carboxypeptidases, acetylcholinesterases, or lipases, the specific functions of the three Abhd proteins are unknown. Previously this Abhd family members included in 'α/β hydrolase' subgroup in the ESTHER

database. These proteins have the α/β hydrolase fold motif and also have a upf0017 protein motif (consensus pattern: D-x(8)-[GN]-[LFY]-x(4)-[DET]-[LY]-Y-x(3)-[ST]-x(7)-[IV]-x(2)-[PS]- x-[LIVM]-x-[LIVM]-x(3)-[DN]-D), which is about 38 to 51 kD protein whose central region contains a number of conserved regions. Now, these Abhd family members newly belong to 'abh_upf0017' subgroup in X-block.

The gene trap strategy using embryonic stem (ES) cells is a powerful method for both the identification of genes and the subsequent establishment of mutant lines (Gossler et al. 1989; Evans et al. 1997). I used a gene-trap vector, pU-Hachi, that carries a *lox*71 site and a *lox*P site (Araki et al. 1999). Structural features of the pU-Hachi vector and scheme of the exchangeable gene trapping are shown in Fig. 5. This vector uses an IRES-β-geo unit as a selection-reporter marker, since it was proved to trap genes whose expression levels in ES cells are very low (Chowdhury et al. 1997; Bonaldo et al. 1998). Since the long IRES-β-geo unit interposed between the *lox*71 and the *lox*P can be easily removed by Cre recombinase (Araki et al. 1997), we can perform plasmid rescue (Niwa et al. 1993; Hicks et al. 1997) to recover the 5'-flanking genomic region as well as the 3'-flanking region (Figs. 5D, 5E). As the *lox*71 site serves as a target for Cre-medited insertion, we can insert a cDNA sequence joined to IRES to express under the trapped promoter (Fig. 5H). The poly(A) signal downstream of the *lox*P plays a role in enhancing the targeted integration event through the poly(A) trap strategy. Since the selection marker gene in a targeting vector dose not have a poly(A) signal, only upon targeted integration

does the selection marker gene fuse to the poly(A) signal on the trap vector, thereby making the cells drug resistant (Fig. 5H).

To search for the genes which are involved in atherosclerosis, I screened mutant mouse lines established by the exchangeable gene trap method utilizing X-gal staining during their embryonic development. One of these lines showed strong reporter gene expression in the vitelline vessels of yolk sacs at embryonic day (E) 12.5. The trap vector was inserted into the *Abhd2* gene, which was shown to be expressed in vascular and non-vascular SMCs of adult mice.

I found that Abhd $^{Gt/Gt}$ mutant mice appear normal without any apparent defect in vascular development. However, they showed both enhanced SMC migration in the explants SMCs culture and marked intimal hyperplasia after cuff placement, suggesting that *Abhd2* negatively regulates the formation of neointimal hyperplasia by inhibiting SMC migration in vascular injury.

Materials and Methodology

2.1. Plasmids

The pU-Hachi vector was derived from pGT1.8IRESβ-geo (kindly provided by Dr. Ausitn Smith, The University of Edinburgh, Edinburgh UK), which contains the SA sequence from the *En-2* gene and β-geo sequence joined to the IRES sequence from the encephalomyocarditis virus (Mountford et al. 1994). First, a *lox*71 *Bam*HI fragment was inserted into the *Bgl*II site of pGT1.8IRESβ-geo. Then, the plasmid, pEBN-SE7ti, was constructed by inserting a 180-bp spacer (SP) sequence, which is part of the rabbit β-globin gene, a *lox*P fragment and the poly A addition (poly(A)) signal from the mouse phosphoglycerate kinase-1 (PGK) gene into the modified pUC19 vector from which the LacZ sequence was removed. The SP sequence was used to protect the 3'-end of the trap vector. pU-Hachi was obtained by introducing a SA-IRES-*lox*71-β-geo *Sal*I fragment into *Sal*I site of plasmid pEBN-SE7ti (Araki et al. 1999).

2.2. Cell Culture and Electroporation

The TT2 (Yagi et al. 1993) ES cell line, which were established from an F1 embryo between a C57BL/6 female and a CBA male (kindly provided by Dr. Shinichi Aizawa, Riken, Japan), was grown as described (Niwa et al. 1993) except for the use of G418-resistant primary mouse embryo fibroblasts as feeder layers. In the case of

electroporation with the pU-Hachi gene trap vector, 100 μg *Spe*I-digested DNA and $3x10^7$ TT2 ES cells were used. The cells were suspended in 0.8 ml of PBS and then electroporated using a Bio-Rad Gene Pulser set at 800V and 3μF, and after 48 hours. They were fed with medium supplement with 200 μg/ml G418. Selection was maintained for 9 days, and then colonies were picked into 24-well plates and expanded for freezing. The trap clones were analyzed by Southern blotting to select cell lines showing a single-copy integration pattern.

2.3. Generation of Gene Trap Mice

The Ayu 8025 gene trap line was isolated as previously described (Araki et al. 1999). Chimeric mice were produced by aggregating ES cells with eight-cell embryos of ICR mice (Clea, Japan). The chimeric male mice were backcrossed to C57BL/6 females to obtain F1 heterozygotes. In this study, we used mice of the F9 generations.

2.4. Cloning of Genomic DNA by Plasmid Rescue

Plasmid rescue was performed to obtain flanking genomic DNA as described (Araki et al. 1999). Briefly, 20 μg of pCAGGS-Cre, a strong Cre expression vector, was electroporated into the trapped ES cells to delete the β-geo cassette through the Cre-mediated recombination between the *lox*71 and the *lox*P. Genomic DNA was prepared from the β-geo-deleted clone, and digested with *Hind*III or *Eco*RV followed

by self-ligation and introduction into E.*coli* by electroporation.

2.5. Southern Blot Analysis and Genotyping of Mice

Southern blot analysis was performed to identify a single integration. Mice tail were lysed with sodium dodecyl sulfate (SDS) /proteinase K, treated with phenol / chloroform, 1:1(vol/vol) twice, precipitated with ethanol, and then dissolved in 10mM Tris-HCL, pH7.5/1mM EDTA(TE). Eight micrograms of genomic DNA prepared from tail biopsies was digested with appropriate restriction enzymes, electrophoresed on a 0.8% agarose gel, and blotted onto a nylon membrane. Hybridization was performed using a DIG DNA Labeling an Detection Kit (Roche, Germany). DNA samples for genotyping were isolated from the tails of embryos, newborn mice and adult mice. Genotyping was done with PCR using tail genomic DNA as a template. For wild-type alleles, a 5' primer, G1 (5'-GAGGTCCTCTGCTCCCTGTAT-3'), located in the deleted region by the trapping event, and a 3' primer, G2 (5'- GTAAGAGCTCCCTTGACTTTCC -3'), located in the 6th exon, were used to generate a 663bp wild-type fragment. To detect the trap allele, another 5' primer, G3 (5'- AGCGGATAACAATTTCACACAGGA-3'), located in the pUC19, and the 3' primer G2 were used to generate a 425bp fragment. For PCR analysis, the DNA was subjected to 30 cycles (30 sec. at 94℃; 60 sec. at 59℃; and, 60 sec. at 72℃) using 0.5 unit of Taq polymerase (Perkin-Elmer, Foster City, CA).

2.6. RNA Analysis

Rapid amplification of cDNA ends (RACE) using the 5' and 3' RACE system (Invitrogen, Carlsbad, California) was utilized to characterize the trapped gene, 5' or 3', as described previously(Oike et al. 1999). Total RNAs were extracted from various tissues and were used for RT-PCR analysis. For northern blot analysis, ten microgram poly(A)+ RNAs isolated from various tissues were purified with the OligotexTM-dT30 mRNA purification kit (TAKARA Shuzo, Kyoto, Japan) and separated on 0.6% agarose gel containing 18% formaldehyde for 4.5 hours and then blotted onto a nylon membrane (Roche, Germany). After baking at 80°C for 1 hour, the membrane was prehybridized with SDS buffer (50% formamide, 0.1% *N*-laurylsarcosine, 2% SDS, 4xSSC, 2% blocking reagent) for 2 h at 68°C, hybridization was performed overnight with an RNA probe was prepared using DIG-labeled antisense probe riboprobes (Roche, Germany) and a detection kit (Roche, Germany). An *Abhd2* specific cDNA (nucleotides 52-550) of RT-PCR fragment was subcloned into pGEM-T vector (Promega, USA) and linearized to transcribe digoxigenin-labeled antisense RNA probe. Primers used in the RT-PCR include the following: A1 (5'- GTTGGACTGCTGGAGTCAAT-3') located in the 1st exon (nucleotide number 48-67); A2 (5'-ACTGCTTCTCGCTGTGGTTG-3') located in the 5th exon (nucleotide number 586-605); B2 (5'-TCCTCTTTGTTAGGGTTCTTC-3') located in the splice acceptor of the trap vector; C1 (5'- GACATATCCCCAGACCCAGC-

3') located in the 6th exon (nucleotide number 763- 782); C2 (5'- ACAGCCGGCTCAAG-3') located in the 8th exon (nucleotide number 1051-1064); D1 (5'- CGACCCCTTGGTGCACGAAAG-3') located in the 10th exon (nucleotide number 1213- 1233); and, D2 (5'- CCAGGGAGAGCCGCCTACTTG-3') located in the 11th exon (nucleotide number 1594-1604). Changes in the mRNA levels of *Abhd2* in the cuff-injured areas were measured by reverse transcriptase-polymerase chain reaction (RT-PCR). The total RNA was extracted from normal and cuff-injured femoral arteries and RT-PCR was performed using two set primers to generate a 432bp fragment: 5'-TCGACCTCTTCGAGCCCCTG-3' located in the 4th exon (nucleotide number 513-532); and, 5'- CCTGCGGCACTGGTC-3' located in the 7th exon (nucleotide number 929-944). Each RNA quantity was normalized to its respective glyceraldehydes-3-phosphate dehydrogenase (GAPDH) mRNA quantity.

2.7. In Situ Hybridization

In situ hybridization analyses were performed on whole mounts and sections of staged embryos as described previously (Kawazoe et al. 2002) and on adult tissue section samples utilized a VENTANA in situ hybridization machine. DIG-UTP-labeled antisense and control sense probe riboprobes (Roche, Germany) were synthesized by transcription from the pGEM-T vector plasmid (Promega, USA) with SP6 or T7 on RNA polymerase and then purified on Quick Spin Columns. (Bio-Rad, Hercules, California)

2.8. Histochemistry, Immunohistochemistory and β-Galactosidase Staining

For immunofluoresecnt detection, tissues were fixed with 4% paraformaldehyde and then washed with three rinses of PBS. Sections were incubated in 4% normal goat serum at room temperature for 1 hour followed by 12-15 hours in a primary antibody solution of PBS/Triton. The α SMA immunoreactivity was detected by an α SMA/HRP monoclonal antibody (Dako Corp.,Carpinteria, CA) diluted 1:500, followed by anti-rat biotin-labeled second antibodies at a 1:500 dilution. The β-galactosidase staining for sample was performed as describe (Yamauchi et al. 1999).

2.9. Preparation of Explants, Proliferation and Migration Assay

Mice aorta explant cultures were performed as described (Kuzuya and Iguchi 2003). Thoracic aorta of adult mice (age 10-12 weeks, wild-type and homozygote mice) were dissected and the endothelium and periadvential fat was removed by gentle abrasion. Then, the aortas were cut into 2 x 2 mm explnts. The explants were individually plated with the lumen side down into collagen type I-coated 12-well multiplates and cultured in 150 μL Dulbecco's modified Eagle's medium (DMEM) containing 10% fetal bovine serum, penicillin/streptomycin and 2-Mercaptoethanol. To characterize the cells migrating from explants, cells were fixed and stained for SM α-actin. For the experiments, SMCs in a subconfluent

state at the 3rd and 5th passage were used.

For the proliferation assay, SMCs were plated on collagen type I-coated 96-well plates ($5x10^3$ cell/well) and then incubated with DMEM containing 0.3% BSA and PDGF-BB (10 ng/mL) (PeproTech EC LTD, UK) for 3days. Cell numbers per well were counted with the use of the Cell Counting Kit-8 (Dojindo, Kumamoto, JAPAN)

The migration assay was performed with Transwell (Corning, Nagog, MA) 24-well tissue culture plates composed of an 8-μm pore polycarbonate membrane. The inner chamber membrane was coated with 0.1% gelatin. SMCs were then seeded on the inner chamber of the Transwell at a concentration of 5×10^3 cells/100μL. The inner chamber was placed into the outer chamber containing recombinant human PDGF-BB (10 ng/mL), and then incubated for 6 hours at 37°C. The cells that migrated onto the outer side of the membrane were fixed and stained. The number of migrated cells was counted in the 5 randomly chosen fields of the duplicated chambers at a magnification of x200 for each sample.

2.10. Cuff –Induced Intimal Thickening of the Mouse Femoral Artery

Ten- to twelve-week-old wild-type and homozygous mice from the same genetic background were used. The cuff placement surgery was performed according to a method and the sections were stained and measured as described (Imai et al. 2002). In brief, the mice were anesthetized by intraperitoneal injection. The

left femoral artery was isolated from the surrounding tissues. A polyethylene tube (PE-50, 2 mm long, inner diameter 0.56 mm, outer diameter 0.965 mm; Becton-Dickinson) was cut longitudinally, loosely placed around the artery, and closed with a suture. After the experimental period, the mice were euthanized, and their arterial tissues were fixed in 10% formalin and then embedded in paraffin. The middle segment of the artery was cut into 5 subserial cross sections at intervals of 200μm. The sections were stained using elactica van Gieson or hematoxylin and eosin staining. The areas of the neointima, media, and adventitia were measured utilizing image-analyzing software (NIH Image). To evaluate DNA synthesis, bromodeoxyurine (BrdU, Sigma-Aldrich, St.Louis, MO) was injected at doses of 100 mg/kg SC and 30 mg/kg IP 18 hours before euthanasia and then at a dose of 30 mg/kg IP 12hours before euthanasia. Immunohistochemistry using anti-BrdU antibody (Dako Corp.,Carpinteria, CA) in serial sections was performed and BrdU index (the ration of BrdU-positive nuclei versus total nuclei) was calculated.

2.11. Statistical Analysis

Values are given as mean ± SEM. All comparisons were done using the Student's *t* test for comparisons between groups. $P<0.05$ is considered significant, and $P<0.01$ was considered highly significant.

Analysis of the Abhd2 Mutant Mice

Results

3.1. Establishment of Ayu8025 Line and Identification of Trapped Gene

First, Araki and colleagues had electroporated the linearlized pU-Hachi vector into TT2 ES cell and isolated 109 trap clones and analyzed their integration patterns of the trap vector by Southern blotting to select those carrying a single copy of the trap vector. Then, 59 % of the clones (64 trap clones) gave a single integrated and retained the *lox*71 site for further analyses. Next, in order to assess the capture of an endogenous gene by the trap vector, the clones were stained with X-gal before and after EB formation. Ninety-seven % of the clones (62 trap clones) showed β-gal activity at undifferentiated ES cell stage and differentiated embryoid bodies stage (day 8), indicating that the use of trap vector pU-Hachi for as an efficient gene trap is available as in the case of other IRES-β-geo vectors.

In order to analyze these trap lines, Araki and colleagues established 36 mouse trap lines through the production of germline chimeras using X-gal positive clones. I screened these mice by whole mount X-gal staining using embryonic and adult stages. Interestingly, one of these lines, Ayu 8025, showed strong expression of *lacZ* in blood vessels such as vitelline vessels (Fig. 6a) embryonic days (E) 12.5 embryos and thus this was further investigated. This mutant mouse line was designated as B6; CB-Abhd2^{GtAyu8025IMEG}. To identify the gene trapped and characterize the

insertion site of the trap vector, I performed 5' RACE and plasmid rescues. The trap vector was inserted into the 5th intron of the *Abhd2* gene. I confirmed that the integration of the trap vector resulted in the deletion of 634 bp of genomic DNA located at nucleotide positions between 63583 and 64216 (Fig. 6b). In addition, 2 bps or 14 bps were deleted from the 5' end or the 3' end of the trap vector, respectively. A tail DNA was used for genotyping by PCR. For the wild type allele, the G1 primer and the G2 primer were used to generate a 663bp wild-type fragment. To detect the trap allele, the G3 primer and the G2 primer were used to generate a 425bp fragment. Using these primers, the genotype of the offspring from the heterozygous inter-cross was easily identified (Fig. 6c). Homozygous mutant mice obtained from the crosses of F1 heterozygotes did not show any obvious abnormalities. They did not exhibit growth retardation, fertile, and took care of their offspring. Heterozygous and homozygous mice appeared normal and were fertile. Even at the 9th backcross generation to C57BL/6, 46 homozygous, 114 heterozygous and 48 wild-type mice were generated among 208 live-born offspring by mating between heterozygote parents (Fig. 6d). This ratio was consistent with the expected Mendelian distribution. Histological analysis did not identify any abnormalities in the main adult organs including the brain, heart, lung, liver, spleen, kidney, skeletal muscle, adrenal gland, testis, uterus, and intestine. The frequency of sudden death in the homozygous mutant mice was not different from that in the wild-type mice within one year.

3.2. Northern Blot and RT-PCR Analyses

To investigate the tissue specific expression and the presence of fusion transcripts, I performed the northern blot analyses on various adult tissues, including brains, hearts, lungs, livers, spleens, skeletal muscles, kidneys, testes, uteruses, and aortas of wild–type, heterozygous and homozygous mice were performed using a fragment of the *Abhd2* cDNA as a probe. In wild-type mice, 6.8 kb transcripts were detected in all tissues examined except for skeletal muscle (Fig. 7a), although the level of expression was variable among these tissues. This 6.8 kb transcript consists of 1.6kb of *Abhd2* ORF and 5.2kb of the 3'UTR region as confirmed by analysis of 3'RACE products. In heterozygous mutant mice, two bands of 6.8 kb and 5.2 kb were detected (Fig. 7a). In homozygous mutant mice, the 5.2 kb transcripts were detected in the same tissues (Fig. 7a) as in the wild type mice. The 5.2 kb transcripts were also hybridized with the *lacZ* probe (Fig. 7a), suggesting that this transcript is a fusion message comprised of 0.5 kb truncated *Abhd2* and 4.7kb *β-geo* mRNA. This was confirmed by sequencing the 5'RACE product.

To examine whether any other alternative splicing product was present or not, RT-PCR analyses were done using probes as described the Materials and Methods. Using probes A1 and A2, 558bp products were detected in wild-type, heterozygous and homozygous mice (Fig. 7b). As expected, 724bp products were only detected in mice carrying the trap alleles when probes A1 and B2 were used (Fig. 7b). When probes C1 and C2 or D1 and D2 were used, 302bp or 392bp products were detected,

respectively, in wild-type and heterozygous mice (Fig. 7b). These results suggest that no other alternative splicing occurs in either the wild-type or trap allele. Thus, the insertion of a trap vector into the 5th intron results in the complete loss of the wild type message and in the transcription of a fusion message. As the fusion message contains up to the 5th exon, it was expected to produce a truncated Abhd2 protein that contains only 180 amino acids of N-terminus, but not the catalytic domain of α/β hydrolase fold protein (Fig. 7c).

3.3. Analysis of X-gal Staining

I examined the cell-type specific expression of the *Abhd2* gene using *lac*Z reporter on the tissue sections of adult mice. It is noteworthy that β-galactosidase activity was detected in vascular SMCs, non-vascular SMCs and the cardiac muscle cells, but not in the skeletal muscle cells. Vascular SMCs include those in the aorta (Fig. 8a, Fig. 9a), femoral artery (Fig. 8b), small arteries in the skin (arrow in Fig. 8c, Fig. 9b), mesenteric artery (Fig. 8d), kidney artery (Fig. 8e and 9i), brain artery (Fig. 8f), arterioles in the ear (arrow in Fig. 9c), and in superior and inferior vena (Fig. 9d). The *lac*Z expression was not detected in veins (arrow head in Fig. 8c, 8d, 9b and 9c), probably because of absence of SMCs. *lac*Z was also expressed in the myocardium of the atrium and ventricles of the heart (Fig. 8g and 9e) and in the non-vascular smooth muscle cells such as the bronchial SMC layers (Fig. 8h and 9f), uterine SMCs (Fig. 9g), intestinal SMC layers (Fig. 8i and 9k), and bladder SMCs (Fig. 8j);

however, *lac*Z was not detected in the skeletal muscle cells (Fig. 9h). We confirmed that X-gal positive cells were indeed vascular or non-vascular SMCs, but not endothelial cells, utilizing immuno-histochemical staining with anti-α-smooth muscle actin antibodies (Fig. 9j and 9l). In-situ hybridization experiments using the *Abhd2* cDNA probe as used for the northern blot analysis (see Fig. 7) revealed that X-gal positive cells were coincident with those cells that expressed the mouse *Abhd2* mRNA (Fig. 9t), suggesting that X-gal staining reflects the *Abhd2* expression pattern.

X-gal positive cells were also detected in other types of cells, such as hepatocytes around hepatic interlobular areas of liver tissue (Fig. 8k and 9m), alveolar type II cells of lung tissue (Fig. 9n), splenic cords (reticular cells) around white pulp in the spleen (Fig. 9o), the cortex area of adrenal gland (Fig. 8i and 9p) and other tissues such as islet cells of Langerhans of the pancreas (Fig. 9q).

3.4. Developmental Expression of *LacZ*

Next, I performed X-gal staining to analyze the developmental expression of *Abhd2* gene on heterozygous embryos. At embryonic day 9.0 (E9.0), weak β-galactosidase expression was detected in the heart and increased gradually from E9.0 to E11.5 (Fig. 10A-a, -b, -c and -d). At E10.5 *lac*Z was expressed in the endothelial cells of the dorsal aorta (Fig. 10B-a), but not in SMCs. This *lac*Z expression in the endothelial cells disappeared by E12.5. In contrast, *lac*Z expression was first detected in SMCs at E11.5 (Fig. 10B-b). At E13.5, *lac*Z was being expressed in

most of SMCs (Fig. 10B-c). By E16.5, *lac*Z was expressed in all SMCs (Fig. 10B-d). Thus, *Abhd2* starts to be expressed in the endothelial cells, and then its expression shifts into SMCs during E10.5 to E13.5.

3.5. Function of *Abhd2 in vitro* and *in vivo*

Although I found that *lac*Z staining showed specific *Abhd2* expression in vascular SMCs, Abhd2$^{Gt/Gt}$ homozygous mutant mice show no phenotype. Thus, we investigated the role of *Abhd2* on the migration and proliferation of vascular SMCs (Fig. 11). SMC's migration from the arterial explants of wild-type mice was observed at about day 4, and migrating cells were detected by 6 day. These migrating cells were X-gal positive (Fig. 12a) and also α SMA immunoreactivity positive. The cell migration from the explants of homozygous mice aortas significantly increased compared with those of wild-type and heterozygous mice ($p<0.01$;Fig. 12b). Next, to analyze the ability of PDGF-BB-directed SMCs to migrate across Transwell filters, an explant culture method with mouse SMCs derived from either wild type or homozygous mutant mice (Fig. 13). I found that the number of cells that passed through the filters in the presence of gradient of chemo-attractant in homozygous mice was 140 ± 22.3 SMCs/field which was significantly higher than the 78.8 ± 17.7 SMCs/field in wild-type mice ($p<0.05$;Fig. 13a).

In the proliferation assay, there was no difference in the PDGF-BB-induced proliferative response of cultured SMCs derived from either wild-type or homozygote

(Fig. 13b). These data suggest that *Abhd2* is involved in the regulation of SMC migration in response to exogenous factors; therefore, I investigated the in vivo role of *Abhd2* on vascular smooth muscles using the cuff placement model. To examine the effect of cuff placement on the neointimal formation, I analyzed histological sections (Fig. 14,15 and 16). In the sham-operated side, no neointimal thickening was found at 7 days or 28 days after surgery in either wild-type or homozygous mice. In the cuff placement side, no neointimal hyperplasia was found at 7 days after surgery in either wild-type or homozygous mice; however, at 28 days after surgery, neointimal hyperplasia was observed in both wild-type and homozygous mice. Neointimal thickening was significantly larger in homozygous mice than in wild-type mice, while the adventitial region was similar between them (Fig. 16a, b). Cells in the neointimal area expressed lacZ and α smooth muscle actin (Fig. 16b).

I examined BrdU uptake assay 7 days after a cuff injury to investigate the proliferative activity of SMCs. BrdU uptakes in both intimal and medial layers were not different between the wild-type or homozygous mice (Fig. 16c). Taken together, neointimal hyperplasia in homozygous mice might be caused by the migration of SMCs, but not by the proliferation of SMCs. If the absence of the *Abhd2* expression is involved in enhanced migration of SMCs, the expression of *Abhd2* should be increased after cuff placement in wild type mice. Thus, we analyzed the time course of *Abhd2* mRNA expression after cuff injury. RT-PCR analysis showed that expression of *Abhd2* increased and reached a maximum level at

7 days after cuff injury (Fig. 16d). These results indicated that the truncated *Abhd2* caused the migration activity of vascular SMCs to enhance, leading to the neointimal hyperplasia after experimental vascular injury.

Discussion

A gene trap Ayu 8025 line was established and showed specific maker gene expression in SMCs in adult mice. I proved that the trap vector of Ayu8025 line was inserted into the 5th intron of the *Abhd2* gene, which is one of the α/β hydrolase protein family numbers. This insertion results in the production of fusion transcript which can produce truncated proteins that contains 180 amino acids, but lacking triad catalytic triad domains (Ser207, Asp345 and His376). Thus, truncated Abhd2 protein may lose its function, however, there is no apparently phenotype of *Abhd2* homozygous mice in normal conditions by F9 generation. The ESTHER, the database of the α/β hydrolase fold superfamily of proteins, reported that mouse Abhd2 protein belongs to the upf_0017 subfamily of the α/β hydrolase fold family including mouse *Abhd1* and *Abhd3* (Hotelier et al. 2004). The mouse Abhd2 protein is related to Abhd1 having 26.8% identity and Abhd3 having 25.3% identity. And the NCBI database just reported the additional data on mouse *Abhd4*, *Abhd5*, *Abhd6*, *Abhd7*, *Abhd8*, *Abhd9*, *Abhd10* and *Abhd11*. However, *Abhd4-11* genes don't have the upf_0017 protein motif. Two genes of this Abhd family have been reported in detail.

First, Lefevre et al. found that eight different mutations in human *ABHD5* gene have been associated with Chanarin-Dorfman syndrome (CDS). CDS is a triglyceride storage disease with impaired long-chain fatty acid oxidation and a rare

autosomal recessive form of nonbullous congenital ichthyosiform erythroderma that is characterized by the presence of intracellular lipid droplets in most tissues (Rozenszajn et al. 1966; Dorfman et al. 1974; Chanarin et al. 1975; Lefevre et al. 2001). Human *ABHD5* been reported to have a homolog of mouse *Abhd5* protein with 94% identity. The proteins encoded by both two genes belong to an α/β hydrolase fold proteins family and contain three sequence motifs that correspond to a catalytic triad. Interestingly, both of two genes differ from other members of this subfamily in that its putative catalytic triad contains an asparagine instead of the usual serine residue. Mouse *Abhd5* was distributed predominantly on the surface of lipid droplets in differentiated 3T3-L1 cells, and its expression increased during adipocyte differentiation. Lipid droplets are a class of ubiquitous cellular organelles that are involved in lipid storage and metabolism. Although the mechanisms of the biogenesis of lipid droplets are still unclear, a set of proteins called the PAT domain family have been characterized as factors associating with lipid droplets. Perilipin, a member of PAT domain family, is expressed exclusively in the adipose tissue and regulates the breakdown of triacylglycerol in lipid droplets via its phosphorylation. Yamaguchi et al. found direct interaction between perilipin and Abhd5 (Yamaguchi et al. 2004).

Second, human *ABHD11* gene encodes a protein containing an α/β hydrolase fold domain. This gene is deleted in Williams-Beuren syndrome, a multisystem developmental disorder caused by the deletion of contiguous genes at 7q11.23.

Williams-Beuren syndrome is a neurodevelopment disorder characterized by congenital heart and vascular disease, hypertension, infantile hypercalcemia, dental abnormalities, dysmorphic facial features, mental retardation, premature aging of skin, and unique cognitive and personality profiles. Alternative splicing of this gene results in six transcript variants, two of which encode the same isoform. The function of this gene is unclear (Morris et al. 1988; Bellugi et al. 1999; Merla et al. 2002). Further study to examine the cell-type specific expression of these family genes will be required to assess the possibility that these genes can compensate for a deficiency of *Abhd2*.

The amino-acid sequence homology to mouse Abhd2 were identified in the folloing other species: *Homo sapiens* (ABHD2, 98.6%), *Pan troglodytes* (XP523148, 99.1%), *Ruttus norvegicus* (predicted-Abhd2, 99.5%), *Gallus gallus* (LOC415493, 91.2%), *Drosophila melanogaster* (CG3488, 43.5%), *Caenorhabditis elegans* (Y60A3A.7.p, 22.7%) and *Saccharomyces cerevisiae* (YMR210W, YPL095c and YBR177c, 24.3%, 22.9% and 23.1%, respectively). All of these proteins have the α/β hydrolase fold motif and the upf0017 protein motif. Mouse Abhd2 has the highest homology to human, chimpanzee and rabbit. Athenstaedt et al. reported that the *S.cerevisiae* mutant strain with a deletion of YBR177c, which is slightly homologous to mouse Abhd2, exhibited mild temperature sensitivity at 37°C but grew better than the wild type at 15°C and the phospholipids composition pattern of mutant strain was significantly different from that of wild-type strain. In this mutant

strain, the cellular levels of phosphatidylinositol and phosphatidic acid were increased at the expense of phosphatidylethanolamine and phosphatidyldimethylethanolamine. And the mutant strain had higher amounts of ergosteryl esters and lanosterol than wild type (Athenstaedt et al. 1999). These results suggested that the gene product of YBR177c was a candidate for involvement in lipid metabolism. An analysis of YBR177c mutant phenotype will be helpful for analyzing the *Abhd2* function and searching for the substrates of Abhd2 protein.

I performed two experiments to study the function of the *Abhd2* gene in vascular SMCs, which expressed *Abhd2* gene abundantly. First, the in vitro study demonstrated that the migratory ability of cultured SMCs from *Abhd2* homozygous mice was higher than that of wild type mice. The proliferation ability showed no significant difference between *Abhd2* homozygous mice and wild type mice. This indicates that *Abhd2* plays a critical role for regulating SMC migration. Second, I investigated the role of *Abhd2* in vivo, using the cuff placement model in the mouse femoral artery. *Abhd2* homozygous mice showed a marked increase in neointimal area in comparison with that of wild-type mice. On the other hand, there was no difference in the PDGF-BB-induced proliferative response of cultured SMCs derived from either wild-type or homozygote in terms of BrdU labeling in either the intimal or the medial region. These results suggest that increased SMC migratory activity is the main cause for the increase of intimal hyperplasia in *Abhd2* deficient mice. However, other growth factors or molecules such as hyaluronic acid, heparin or

aminoglycan chains of heparan sulfate proteoglycans also affect SMC's migration and proliferation after vascular injury is reported. Savani et al. reported that SMCs secrete a hyaluronic acid into extracellular matrix and hyaluronic acid was involved vascular injury model (Savani et al. 1995). Papakonstantinou et al. reported that hyaluronic acid plays a role of positive regulator on the PDGF-BB induced SMC proliferation (Papakonstantinou et al. 1995; Papakonstantinou et al. 1998). To investigate the roles of these molecules and the extracellular matrix, further studies will be required.

I described a mouse model of vessel injury that was induced by placing a nonocculsive cuff around the femoral artery. This model has been described and characterized in rabbits (Booth et al. 1989; Kockx et al. 1993). To address questions relevant to vascular biology and atherosclerosis, Mori et al. adapted this model to transgenic mice (Moroi et al. 1998). In cuff model, the endothelial cells are not directly manipulated or removed, allowing study of the effect of individual endothelial factors. The mechanism of neointimal formation after cuff placement is not known yet. Previous studies have been reported that medial SMCs are modified and migrate into the intima, where they proliferate and secrete extracellular matrix components (Newby and Zaltsman 2000), and that adventitial fibroblasts migrate into the neointima and differentiate into SMC-like cells (Zalewski and Shi 1997). Recently, Tanaka et al. (2003) reported that in the cuff placement model bone marrow-derived cells are seldom detected in the neointima, whereas many

inflammatory cells in the adventitia are derived from bone marrow cells (Tanaka et al. 2003). Yang et al. (2004) also found that the neointimal formation was caused by an interaction and differentiation between macrophages and SMCs in the adventitia area (Xu et al. 2004). From these studies, it is not certain that neointimal cells, which express *Abhd2*, migrate from adult bone marrow.

Several α/β hydrolase protein family numbers have been reported to associate with the pathogenesis of atherosclerosis. N-myc downstream regulated gene 4 (Ndrg4), also known as smooth muscle-associated protein 8 (smap8), belongs to the α/β hydrolase protein family members as predicted from nucleotide sequences and was expressed in moderate amounts in vascular smooth muscle cells. Nishimoto et al. showed that homocysteine induced highly *Ndrg4* expression in vascular SMCs. Homocysteine, a sulfur-containing amino acid, is an intermediate metabolite of methionine and is widely recognized as an independent risk factor for atherogenesis (Malinow et al. 1998; Nishimoto et al. 2003), because patients with severe homocysteinemia suffer from arterial and venous thromboembolic events at an early age. Although overexpression of *Ndrg4* decreased the proliferation and migration of rat aortic smooth muscle cells (A10 cells), PDGF-induced proliferation was significantly enhanced in *Ndrg4* expressed cells. These results suggest that *Ndrg4* is involved in the regulation of mitogenic signaling in vascular SMCs, possibly in response to a homocysteine-induced injury. Soluble epoxide hydrolase (sEH, previously called cytosolic epoxide hydrolase) plays a role to detoxify a large variety

of xenobiotic-derived epoxides and one of its substrates is epoxyeicosatrienoic acids (EETs), which are synthesized by endothelial cells, and taken up by vascular SMCs. EETs control vascular tone and contribute to pathogenesis of atherosclerosis. sEH is critical in the control of EET levels and inhibitors of sEH have been reported to attenuate vascular SMC proliferation (Chacos et al. 1983; Fang et al. 1996; Rosolowsky and Campbell 1996; Davis et al. 2002); furthermore, the human polymorphism of sEH has been reported to be associated with atherosclerosis (Fornage et al. 2004). Chen et al. cloned retinoid-inducible serine carboxypeptidase (RISC) from vascular SMCs as a target molecule by retinoids. Retinoids are involved in the vascular response to injury and blocks SMC proliferation and attenuates neointimal hyperplasia formation after injury (Axel et al. 2001). From these studies, these α/β hydrolase proteins suggest to be involved in the behavior of vascular SMC and the progression of atherosclerosis.

I found that *Abhd2* was expressed in alveolar type II cells of the lung and hepatocytes around the interlobular area of the liver. Three *Abhd* family genes were identified in a gene expression screen of human emphysematous tissue (Edgar and Polak 2002). The *Abhd2* expression of alveolar type II cells suggests that *Abhd2* associates with the lung homeostasis and the process of emphysema. Actually, microsomal epoxide hydrolase, one of α/β hydrolase protein family numbers, was expressed in the alveolar epithelial cells including alveolar type II cells (Takeyabu et al. 2000) and is associated with the genetic susceptibility for the development of

emphysematous changes of the lung (Smith and Harrison 1997). In addition, abnormalities in the surfactant homeostasis of alveolar type II cells cause the emphysematous change (Sulkowska et al. 1996). My result suggests that *Abhd2* in alveolar type II cells keeps alveolar tissues in normal homeostasis and protects from progressive emphysema, however adult *Abhd2* homozygous mice showed no significant structural change in lung tissue. The hepatocytes in the liver are quite heterogeneous in terms of the blood supply. The interlobular and centrilobular hepatocytes receive different signals owing to the decrease of substrate concentrations including O_2 and hormone levels during passage of blood through the liver sinusoids. Hepatocytes located in the interlobular zone differ from those in the centrilobular zone. In general, the capacity for oxidative energy metabolism, urea synthesis, bile formation, cholesterol synthesis and cell protection is higher in the interlobular zone and xenobiotic metabolism is higher in the centrilobular zone (Thurman and Kauffman 1985; Kietzmann and Jungermann 1997). Glucose 6-phosphatase, fructose 1,6-bisphosphatase, phosphoenolpyruvate carboxykinase were higher activities in the interlobular zone and, conversely, glucokinase and pyruvate kinase were higher activities in the centrilobular zone. The interlobular hepatocytes have higher capacity for glucose output, whereas the centrilobular hepatocytes have higher capacity for glucose uptake. *Abhd2* was expressed more strongly around portal veins at the interlobular zone, suggesting that *Abhd2* at the interlobular zone protects hepatocytes against exogenous stress factors. Further investigation, such as

smoke inhalation experiments or drug administrations, may clarify the function of *Abhd2* in the lung or liver.

Rapidjko et al. cloned human *ABHD2* (*PHPS1-2*) from human placental cDNA (Rapiejko et al. 1988), demonstrating that primary structure of a human protein bears structural similarities to members of the rhodopsin /β-adrenergic receptor family. Human *ABHD2* was structurally similar to mouse *Abhd2* protein with 98.6% identity and its function is not identified yet. The comparison of mouse *Abhd2* and human *ABHD2* protein sequence indicates that both triad catalytic triad domains (Ser, Asp and His) are conserved and the number of difference amino acid are five (Fig. 17). From these report and database, human *ABHD2* might have similar biological function as that of mouse *Abhd2*. From the analysis of mouse *Abhd2*, we will be able to elucidate the role of human *ABHD2* in vascular diseases or emphysematous disease and to apply this knowledge to the diagnosis and treatment of vascular diseases, such as vascular remodeling: atherosclerosis and post-angioplasty restenosis. And genetic analyses such as linkage or association studies using polymorphic makers might be useful to assess whether the human *ABHD2* gene can be a risk factor for atherosclerosis disease, post-angioplasty restenosis and also emphysematous disease.

In conclusion, we find that *Abhd2* is involved in the migration of vascular SMC under the pathologic condition, indicating that *Abhd2* plays an important role in stress response to external stimulation. Identification of substrates for *Abhd2* will provide

an important clue for elucidating the molecular mechanisms of SMC migration and of human vascular diseases.

Figure Legends

Figure 1. Stage of Atherosclerosis

(a) Endothelial dysfunction in atherosclerosis. The earliest changes that precede the formation of lesions of atherosclerosis take place in the endothelium. (b) Fatty-Streak Formation in atherosclerosis. Fatty streaks initially consist of lipid-laden monocytes and macrophages (foam cells) together with T lymphocytes. Later they are joined by various numbers of SMCs. The steps involved in this process include SMC migration, which is stimulated by PDGF, bFGF, and TGFβ.

(c) Formation of an advanced, complicated lesion of atherosclerosis. As fatty streaks progress to intermediate and advanced lesions, they tend to form a fibrous cap that walls off the lesion from the lumen. The fibrous cap covers a mixture of leukocytes, lipid, and debris, which necrotic core. (d) Unstable fibrous plaques in atherosclerosis. Rupture of the fibrous cap or ulceration of the fibrous plaque can rapidly lead to thrombosis and usually occurs at sites of thinning of the fibrous cap that covers the advanced lesion. (Ross R. Engl J Med 1999; 340:115-126)

Figure 2. Secondary structure diagram of the 'canonical' α/β hydrolase fold

Canonical α/β hydrolase fold: an α/β sheet of five to eight β-sheets connected by α-helices to form an α/β/α sandwich. The structure of this protein has a nucleophile-histidine-acid catalytic triad, the elements of which are borne on loops which are the best-conserved structural features in the fold (red arrows).

Figure 3. The Relationship of These Protein Subfamilies

The α/β hydrolase fold group of sequences includes cholinesterases / carboxylesterases group (C-Block), lipase group (L-Block), hormone sensitive lipases (H-Block) and all other protein (X-Block).

Figure 4. Dendrogram of the Relatedness of Other Members of Protein Family to the Mouse Abhds

Dendrogram showing the relatedness of other members of this protein family to mouse Abhds. The predicted relationships were obtained using the Clustal algorithm and drawn using Treeview. The length of the horizontal lines indicates the closeness of the relationships. The spices are: Hs, *Homo sapiens*; Mm, *Mus musculus*; Dm, *Drosophila melanogaster*; Ce, *Caenorhabditis elagans*; At, *Arabidopsis thaliana*; Pg, *Picea glauca*; Sc, *Saccharomyces Cerevisiae* and Ec. *Escherichia coli.*

(Edgar et al. Biochem Biophys Res Commun 2002,292(3): 617-25)

Figure 5. Exchangeable Gene Trapping System

To induce a mutation by introducing the trap vector, pU-Hachi, and then use the established clones, we get any types of mutation by inserting another DNA fragment into the *lox*71 site in the trap vector through Cre-mutant *lox* recombination. After the production of chimeric mice and germ line transmission, both resulting phenotypes *in vivo* can be analyzed. The thick bars under the map indicate the proves used in Southern blotting, and the small arrows indicate the positions and directions of the PCR primers. B: *Bam*HI; P: *Pst*I; E: *Eco*RI; X: *Xho*I; H: *Hind*III; S: *Sph*I.

Figure 6. Insertional Mutation of *Abhd2* Gene

a. Expression of *lac*Z at E12.5. X-gal is positive for vitelline vessels in the yolk sac and other tissues including somites. b. Structure of the wild type and trap alleles. The trap vector, pU8, was inserted into the 5th intron of the *Abhd2* gene, resulting in a loss of 0.6kb intronic sequences. The red arrowheads, G1, G2, and G3, are used for the genotyping of mice. Black arrowheads, A1, A2, B2, C1, C2, D1, D2, Neo1, and Neo2 are used for RT-PCR. c. PCR genotyping. The wild type or trap allele is detected using G1 and G2 or G1 and G3 primer sets, respectively. +/+: wild type mouse, +/Gt: heterozygous mutant mouse, Gt/Gt: homozygous mutant mouse. d. Genotype was determined by PCR analysis of genomic DNA prepared from tails of adult mice. This ratio was consistent with the expected Mendelian distribution.

Figure 7. Disruption of *Abhd2* Expression in Mutant Mice

a. Northern blot analyses of wild type (+/+), heterozygous (+/Gt), and homozygous mutant (Gt/Gt) mice. In the +/+ mouse, only a 6.8 kb band was detected in various tissues. In the +/Gt mouse, both 6.8kb and 5.2 kb bands were detected. In the Gt/Gt mouse, only a 5.2 kb band which was hybridized with both *Abhd2* and *lacZ* probes was detected. These result suggest that the insertion of trap vector results in the complete loss of wild type mRNA and in the production of 5.2kb fusion mRNA.

b. RT-PCR analyses using primers shown in Fig. 1b. Using probes A1 and A2, 558 bp products were detected in +/+, +/Gt and Gt/Gt mice. Using probes A1 and B2, 724 bp products were only detected in mice carrying the trap allele. When probes C1 and C2 or D1 and D2 were used, 302 bp or 392 bp products were detected, respectively, in +/+ and +/Gt mice, but not in Gt/Gt mouse. These results suggest that no other alternative splicing occurs in either the wild-type or the trap allele. c. Schematic diagram of wild-type and truncated Abhd2 protein. Truncated Abhd2 protein lacks most of α/β hydrolase fold domain. Arrowheads indicate triad catalytic domains (Ser207, Asp345 and His376). M: size marker; Br: brain; He: heart; Lu: lung; Li: liver; Sp: spleen; In: intestine; Ki: kidney; Te: testis.

Figure 8. Whole mount of X-gal Staining in Heterozygous Mice

LacZ expression was detected in the aorta (a), femoral artery (b), small artery and vein in the skin (c), mesenteric artery and vein (d), arcuate arteries and interlobular arteries in the kidney (e), and artery surface of the brain (f). *LacZ* was also expressed in the myocardium of the atrium of the heart (g) and non-vascular smooth muscle cells, such as the bronchial tract (h), intestinal tube (i) and urinary bladder (j). X-gal positive cells were detected in other types of cells, such as the liver tissue (k) and the adrenal gland (l). A: Artery; V: vein.

Figure 9. Section of X-gal Staining in Heterozygous Mice

LacZ expression was detected in vascular SMCs of the aorta (a), small arteries in the skin (arrow in b), arterioles in the ear (c), superior and inferior vena (d), but not in veins (arrowheads in band c). *LacZ* was also expressed in the myocardium of the atrium and in the ventricle of the heart (e) and non-vascular smooth muscle cells, such as the bronchial SMC layer (f), uterine SMCs (g), and intestinal SMC layer (k); however, *lacZ* was not detected in skeletal muscle cells (h). X-gal positive cells are clearly stained with anti-α-smooth muscle actin antibody in both vascular (j) or non-vascular tissues (l). X-gal positive cells were also detected in other types of cells, such as the hepatocytes around hepatic interlobular area of liver tissue (m), alveolar type II cells of lung tissue (n), splenic cords (reticular cells) around white pulp in the spleen (o), the cortex area of the adrenal gland (p), and the islet of Langerhans of the

pancreas (q). In situ hybridization section of coronary artery using by Abhd2 probe (r). A: Artery; V: vein; IT: intestinal tract; IV: interlobular vein; CV: central vein; RP: red pulp; WP: white pulp; ZG: Zona glomerulosa; ZF: Zone faciculata; L: islet of Langerhans. Scale bar = 100 μm

Figure 10. Developmental Expression of *LacZ* in the Aorta

A, Specific expression of the *Abhd2* gene in vascular system and other organs in heterozygous embryos. These whole embryo of *LacZ* staining illustrated are E9.0(a), E9.5(b), E10.5(c), E11.5(d). B, At E10.5, *lac*Z was expressed in endothelial cells of the dorsal aorta, but not in SMCs (a). At E11.5, *lac*Z expression was detected in both endothelial cells and in SMCs (b). At E13.5, *lacZ* was expressed in most of the SMCs (c). At E16.5, *lac*Z was expressed in all SMCs, but in only a few endothelial cells (d). Thus, the expression of *Abhd2* starts in endothelial cells, and then shifts to SMCs during embryonic development. Arrowheads indicate the lacZ positive cells. Scale bar = 25 μm.

Figure 11. Preparation of Smooth Muscle Cell Explants and Migration Assay

Thoracic aortas of adult mice were dissected and the endothelium and periadvential fat was removed by gentle abrasion. Then, the aortas were cut into 2 x 2 mm explnts. The explants were individually plated with the lumen side down into collagen type I-coated multiplates and cultured in DMEM containing 10% FBS,

antibiotics and 2-ME. For the experiments, SMCs in a subconfluent state at the 3rd and 5th passage were used. The migration assay was performed with Transwell 24-well tissue culture plates composed of an 8-μm pore polycarbonate membrane. SMCs were then seeded on the inner chamber of the Transwell at a concentration of 5 x 10^3 cells/100μL. The inner chamber was placed into the outer chamber containing recombinant human PDGF-BB, and then incubated for 6 hours at 37°C. The cells that migrated onto the outer side of the membrane were fixed and stained.

Figure 12. LacZ Stain of Explant SMC and Cultured SMC Migration

(a) Cell migration from the arterial explants of heterozygous mice. Cultured SMC was X-gal positive. (b) On explant culture after 10 days, many migrating SMCs were observed and the area of migration border line (red line) around explant was measured. (c) The cell migration from the explants of homozygous mouse aortas significantly increased compared with those of wild-type and heterozygous mouse ($p<0.01$ vs wild type or heterozygous). Explant SMCs was cultured in the DMEM containing 10% FBS, antibiotics and 2-ME. Quantitative analysis of the area of explant culture was performed with the NIH Image software. Results represent mean ± SEM of 8 experiments.

Figure 13. Function of *Abhd2 in vitro*

Cultured SMCs derived from the aortas of wild-type and *Abhd2* deficient mice were used for experiments. (a) Transwell assay for SMC migration in the presence of PDGF-BB. The number of cells that passed through the filters in the presence of PDGF-BB (10 ng/ml) in homozygous (Gt/Gt) mice was 140±22.3 SMCs/field which was significantly higher than 78.8±17.7 SMCs/field in the wild-type (+/+) mice ($p<0.05$). (b) Proliferative ability of SMCs from wild-type or homozygous mice. Data are expressed as a percentage of the cell number in SMCs incubated with culture medium without PDGF-BB. There was no difference in the PDGF-BB-induced proliferative response of cultured SMCs derived from wild-type or homozygous mice. Results represent mean ± SEM of 8 experiments. ** P<0.01e.

Figure 14. Cuff Placement Method

The femoral artery was isolated from the surrounding tissues. Then the femoral vein and nerve were separated from the femoral artery. A polyethylene tube was cut longitudinally, loosely placed around the artery, and closed with a suture.

Figure 15. Cuff Placement 21 Days After Operation

On 21 days after cuff placement, the mice were euthanized, and the femoral artery was isolated from the surrounding cuff placement (a). Tissues were fixed in 10% formalin and embedded in paraffin. The sections were stained by Elastica van Gieson or hematoxylin and eosin staining (b).

Figure 16 Function of *Abhd2 in vivo*

(a)The intimal/media ratio at 28 days after cuff placement. Intimal/media ratio was significantly larger in homozygous mice than in wild-type mice.

(b) Sections of the femoral arteries 28 days after cuff placement of wild-type and homozygous mice stained with Elastica van Gieson, X-gal and anti-αSMA antibody. Neointimal thickening was significantly larger in homozygous mice than in wild-type mice, while the adventitial region was similar between them. Cells in the neointimal area expressing *lacZ* (blue) and α smooth muscle actin (blue) are indicated by arrowheads. (c) BrdU uptakes in both the intimal and the medial layers. BrdU uptakes in both intimal and medial layers were not different between the wild-type and homozygote mice. (d) Time course of *Abhd2* mRNA expression after cuff placement. Expression of *Abhd2* increased and reached a maximum level at 7 days and then decreased to an undetectable level by 14 days after cuff placement of the femoral artery. Glyceraldehyde-3-phosphate dehydrogenase (GAPDH) was used as an internal control. Quantitative analysis of the area of intimal/media was

performed with the NIH Image software. Results represent mean ± SEM of 8 experiments. ** P<0.01e.

Figure 17. Mouse *Abhd2* and Human *ABHD2* Homology

Comparison of Mouse *Abhd2* and Human *ABHD2* protein sequence. Both triad catalytic triad domains (Ser, Asp and His) are conserved (gray boxes).

Figure. 1 Stage of Atherosclerosis

(a)

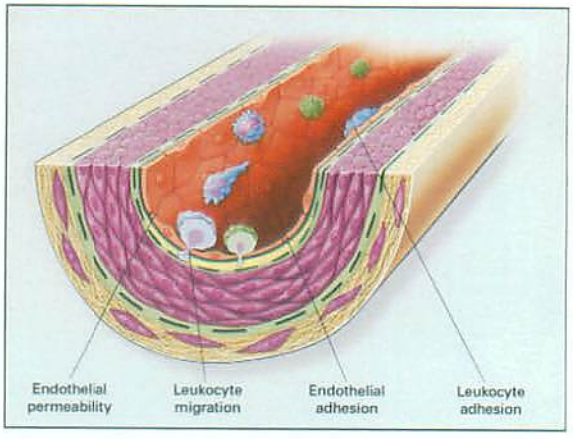

(b)

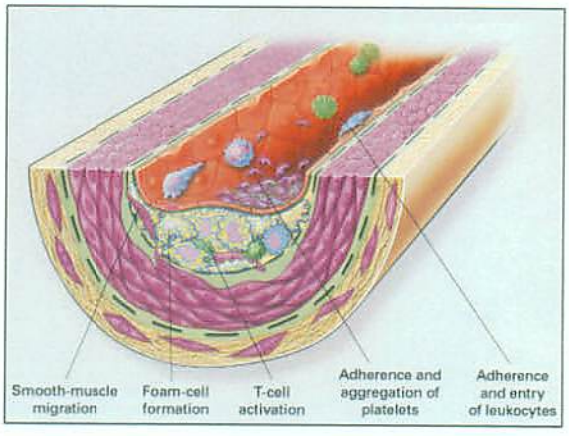

(c)

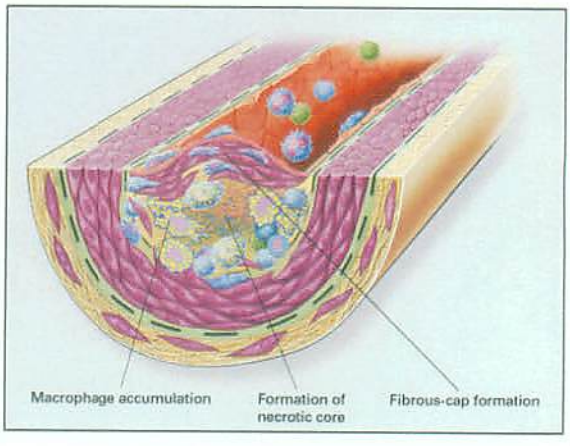

(d)

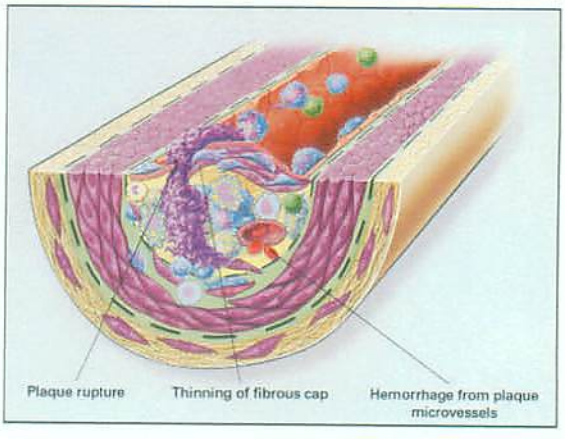

(Ross RN. Engl J Med 1999)

Figure. 2 Secondary structure diagram of the 'canonical' α/β hydrolase fold

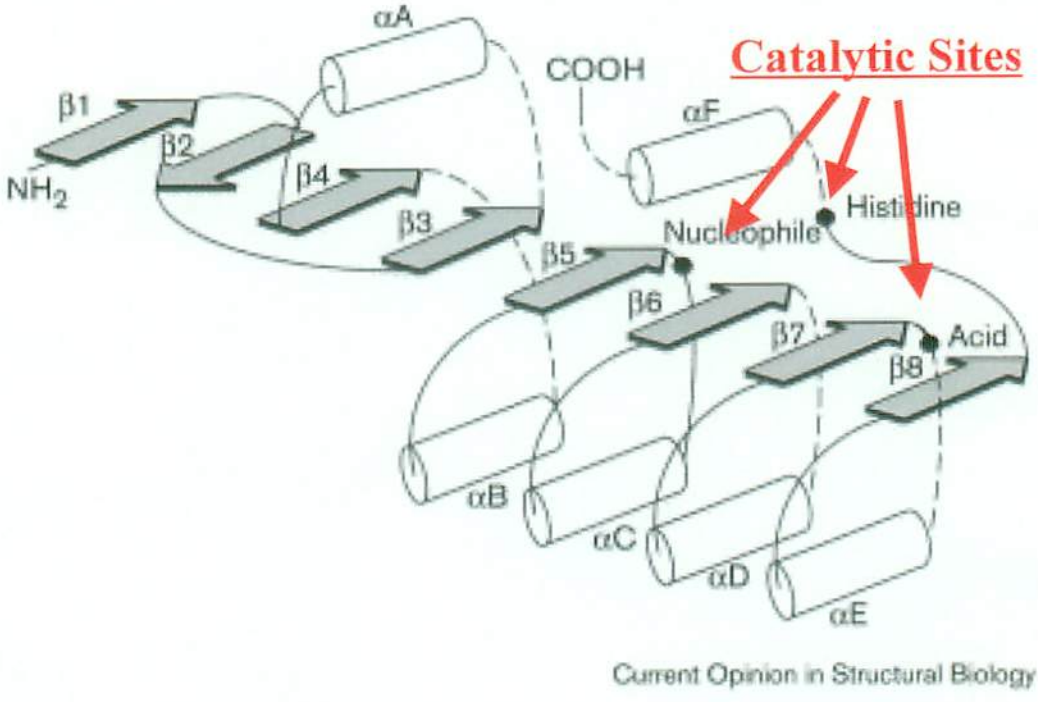

Figure. 3 The Relationship of These Protein Subfamilies

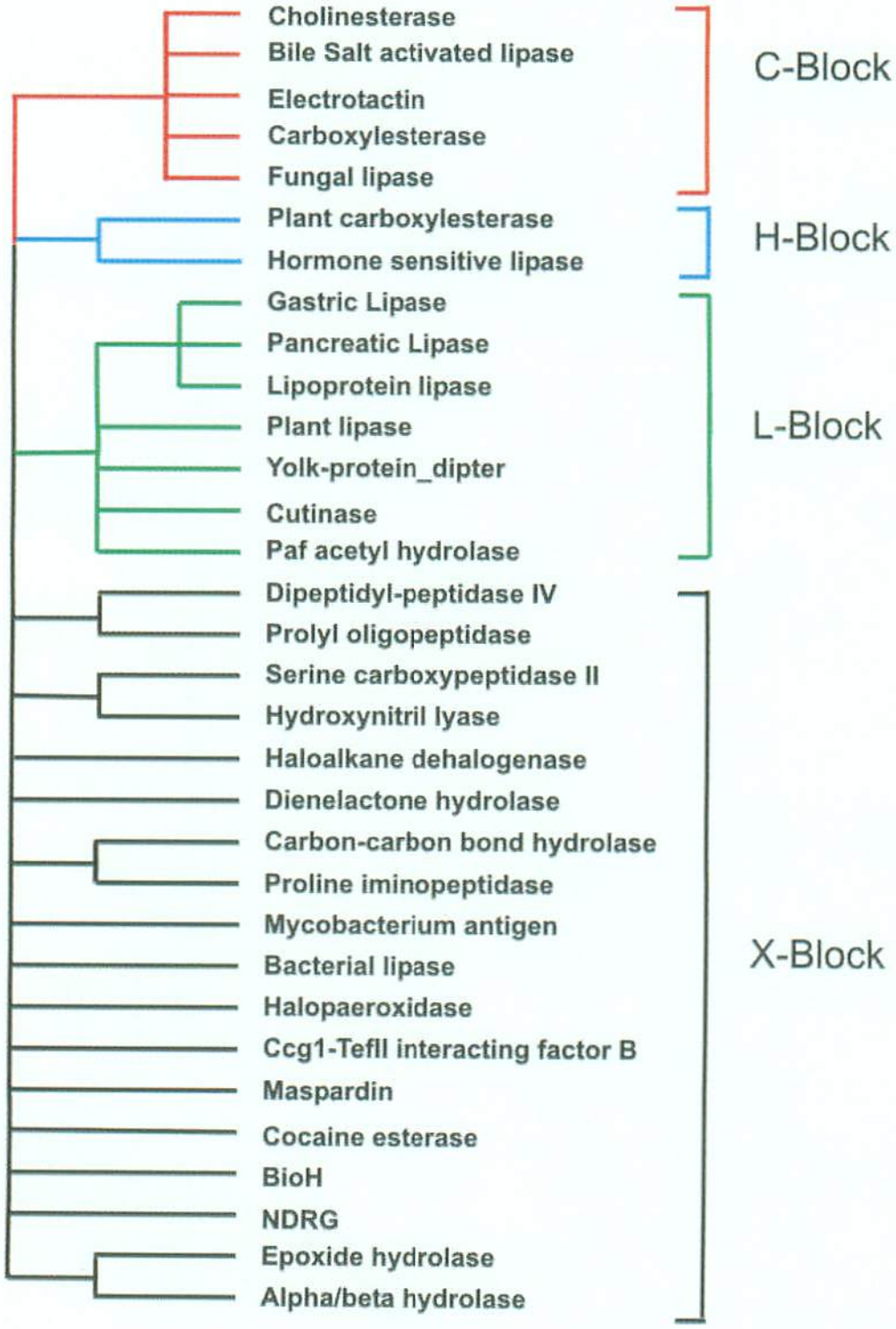

Figure. 4 Dendrogram of the Relatedness of Other Members of Protein Family to the Mouse ABHDs

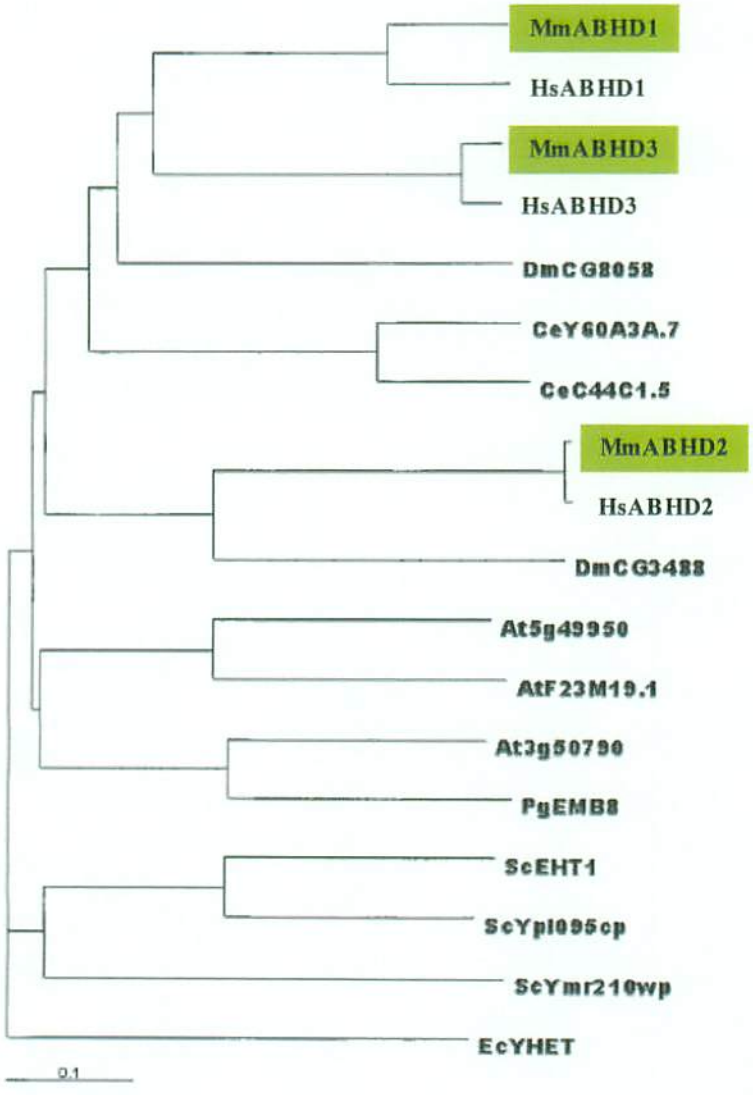

(Edgar et al. Biochem Biophys Res Commun 2002)

Figure. 5 Exchangeable Gene Trapping System

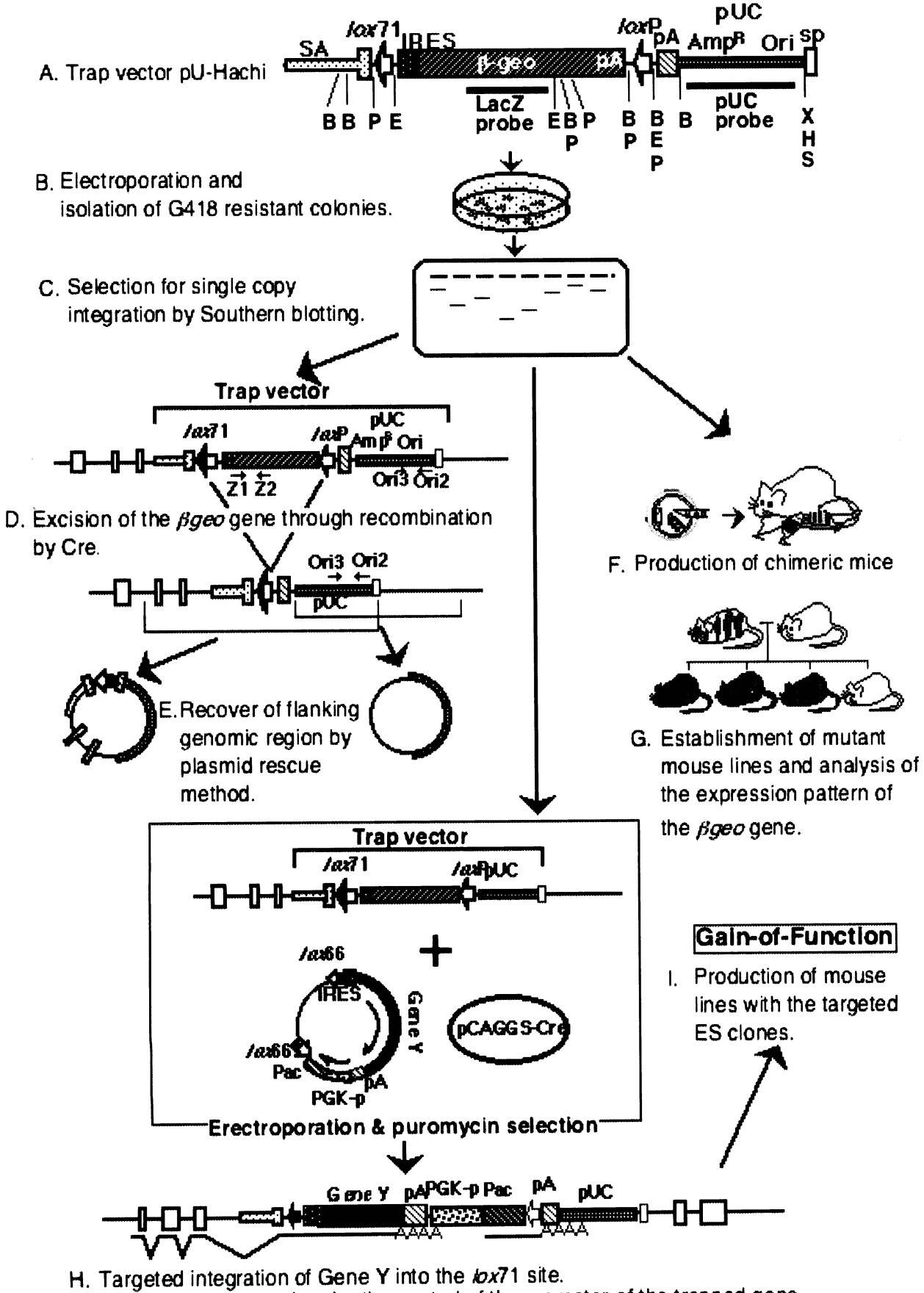

Figure. 6 Insertional Mutation of *Abhd2* Gene

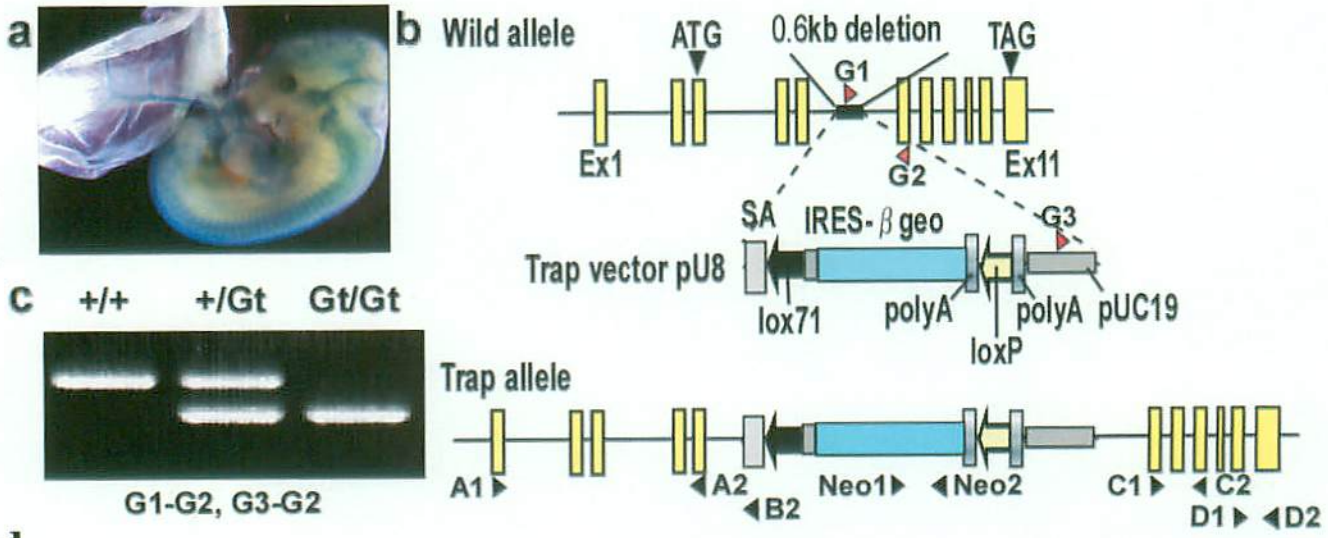

d

Birthday	+/+	+/-	-/-	*Total*
male	16	52	21	89
%	18.0%	58.4%	23.6%	100%
female	32	62	25	119
%	26.9%	52.1%	21.0%	100%
total	23.1%	54.8%	22.1%	100%

Figure. 7 Disruption of *Abhd2* Expression in Mutant Mice

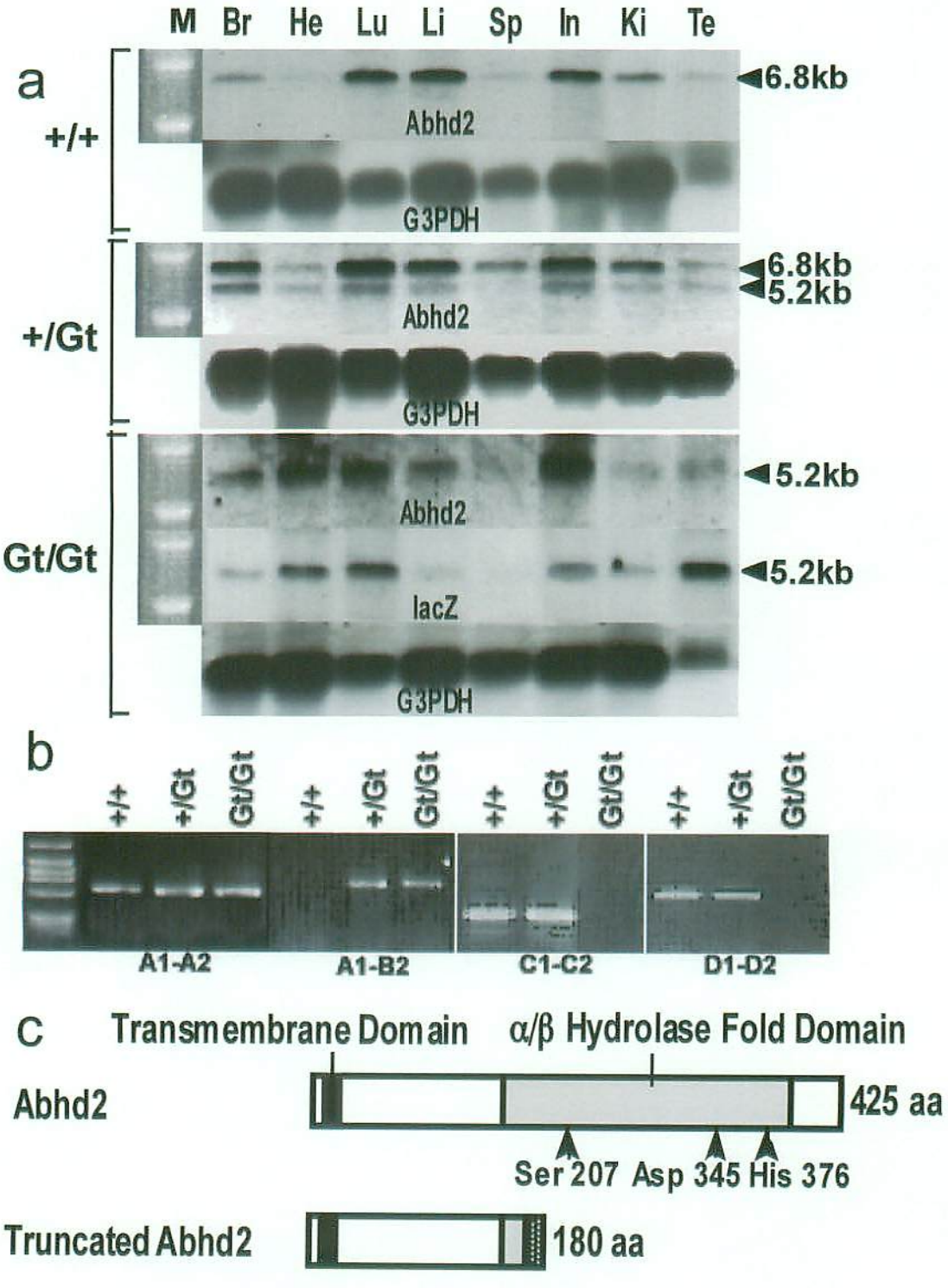

Figure. 8 Whole mount of X-gal Staining in Heterozygous Mice

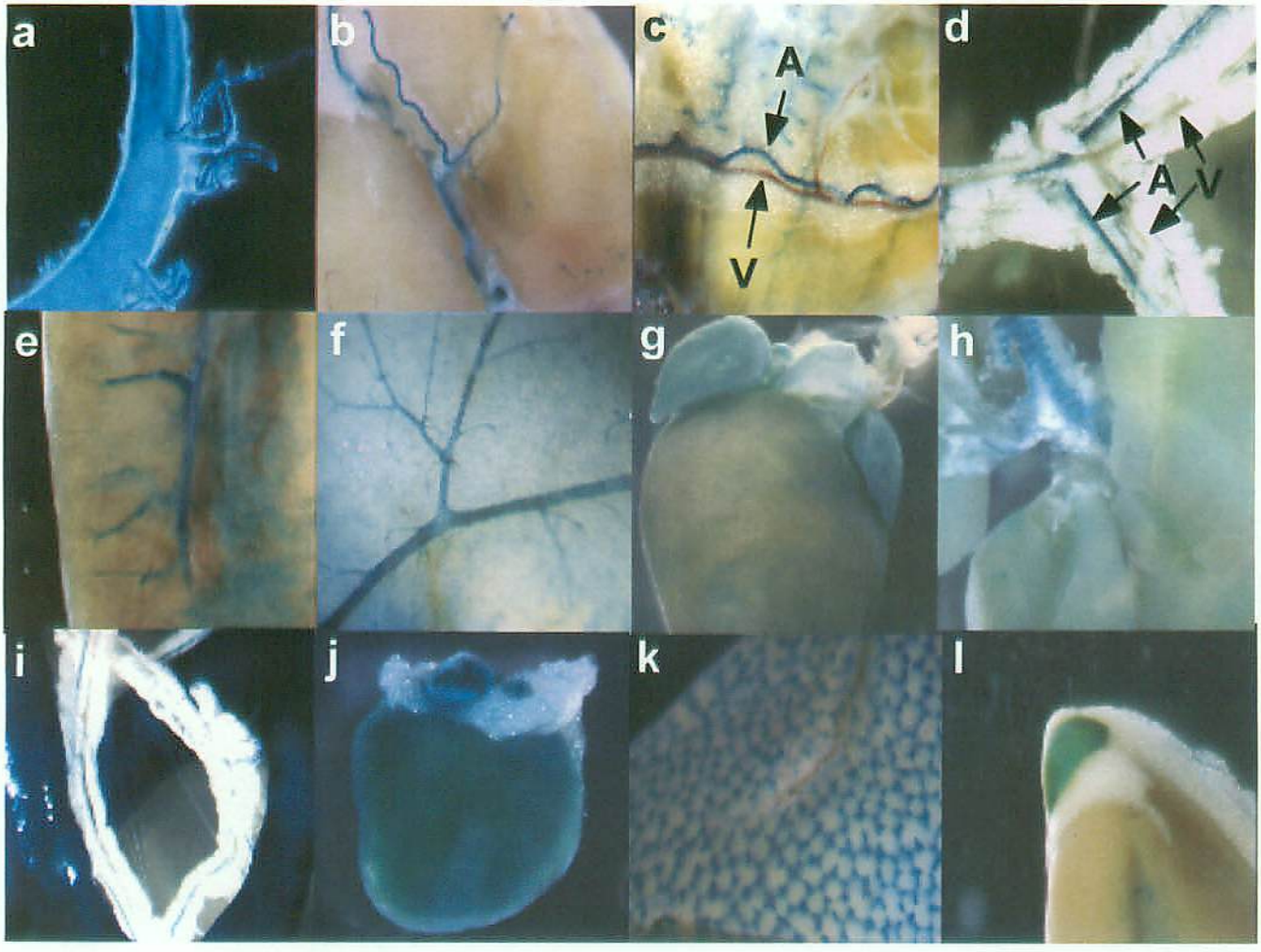

Figure. 9 Section of X-gal Staining in Heterozygous Mice

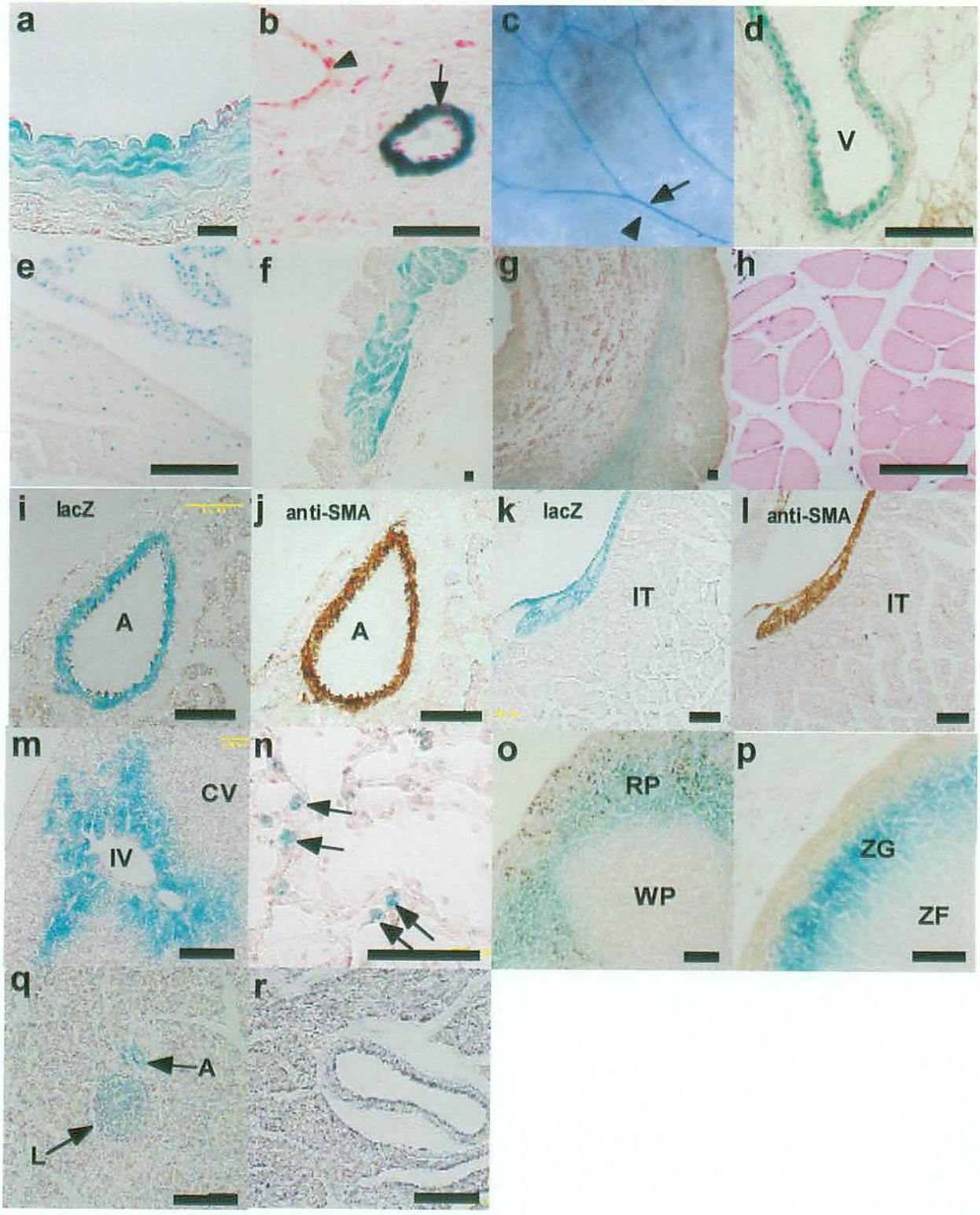

Figure. 10 Developmental Expression of *LacZ* in the Aorta

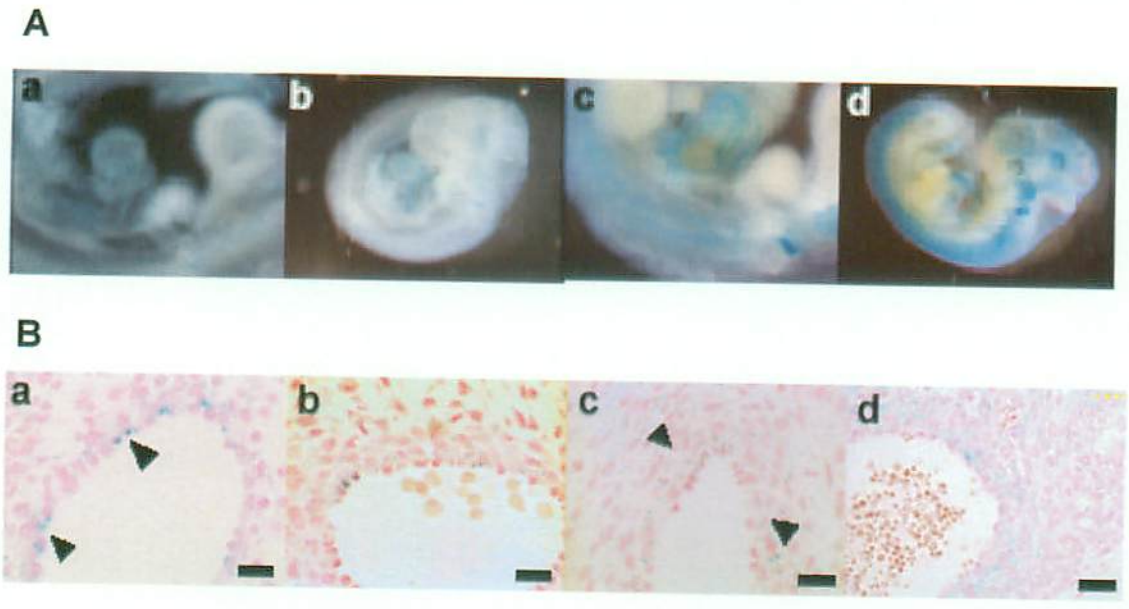

Figure. 11 Preparation of Smooth Muscle Cell Explants And Migration Assay

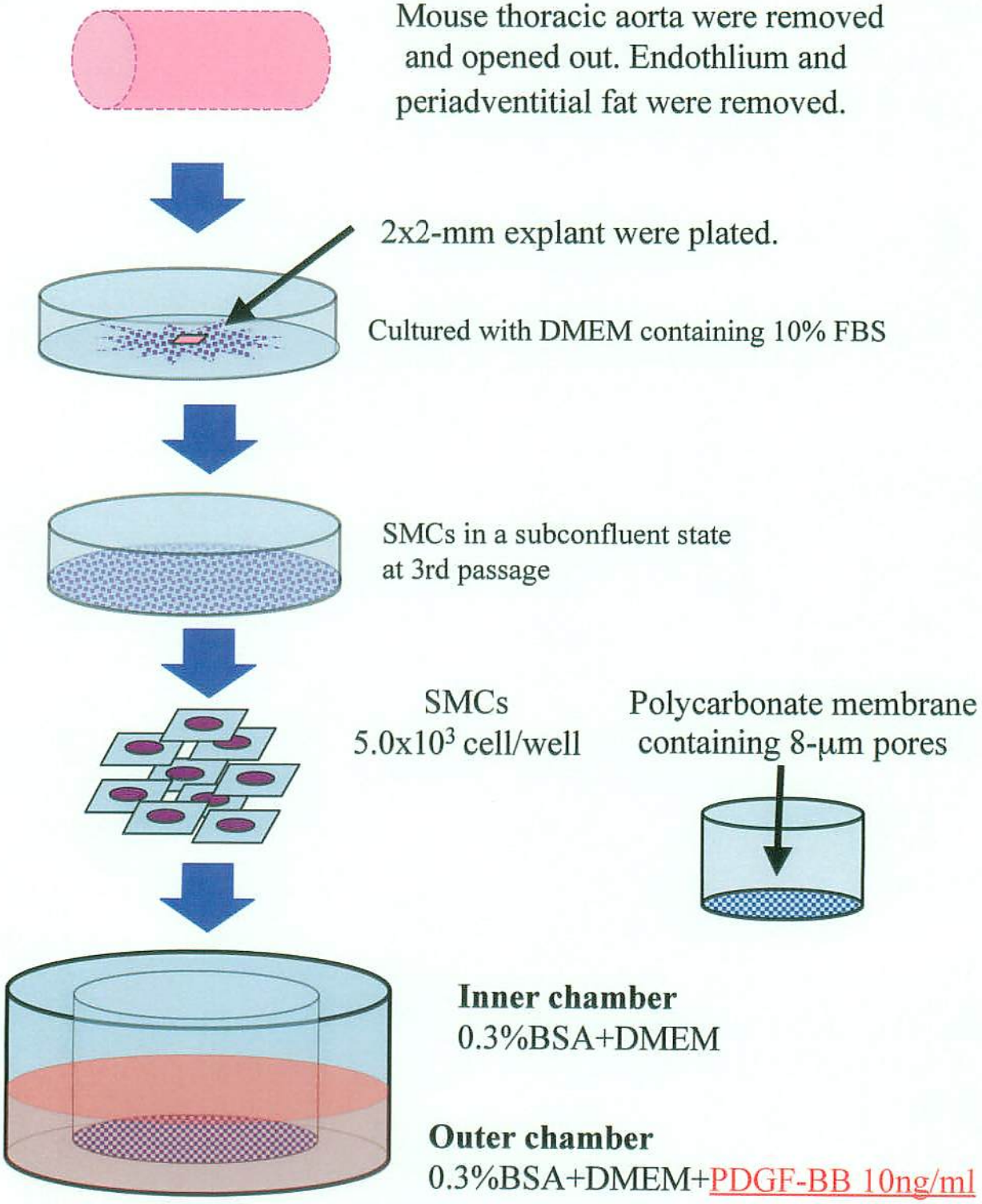

Figure. 12 LacZ Stain of Explant SMC and Cultured SMC Migration

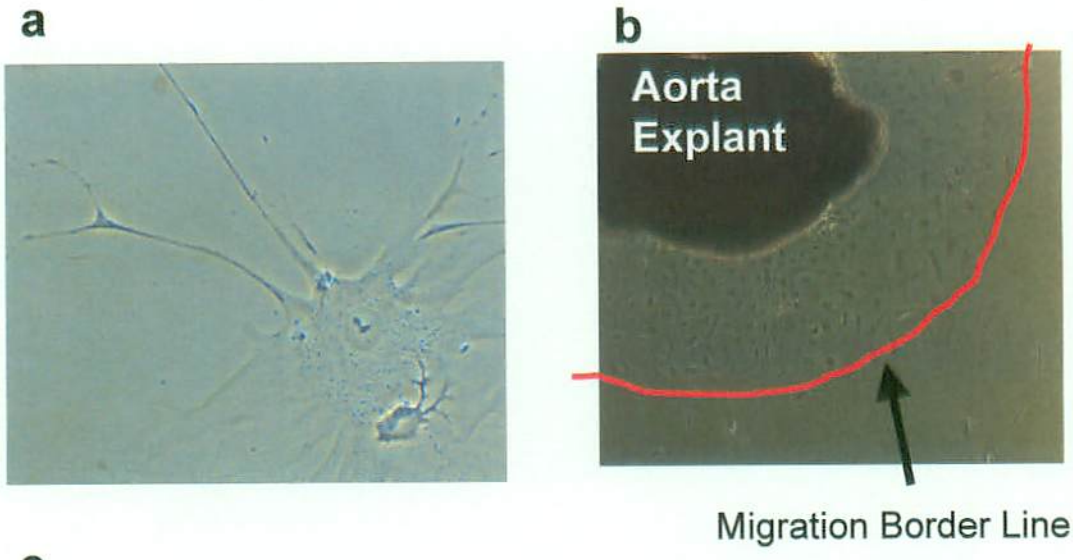

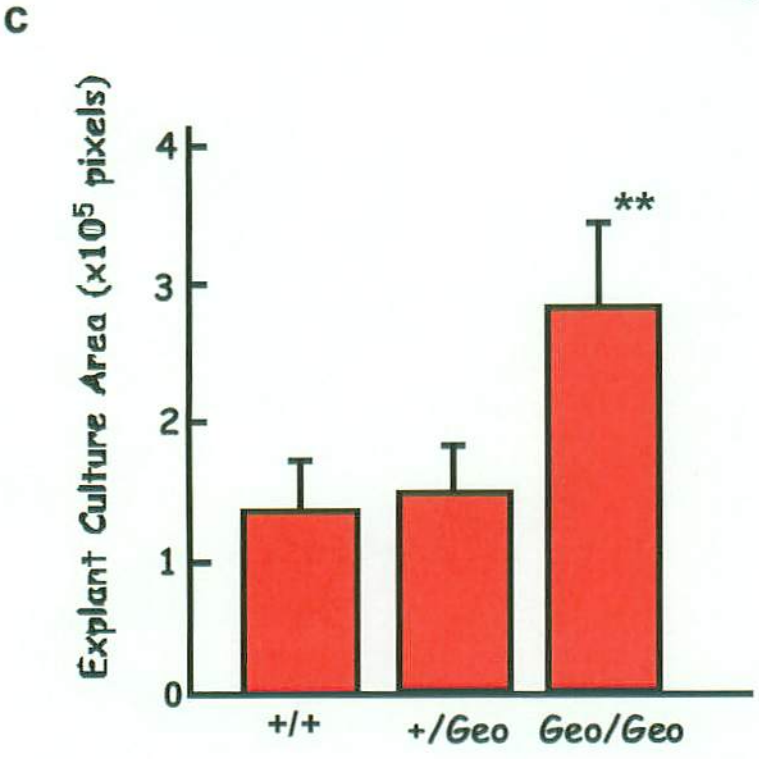

(n=8 ;** p<0.01 vs +/+ and +/Geo)

Figure. 13 Function of *Abhd2 in vitro*

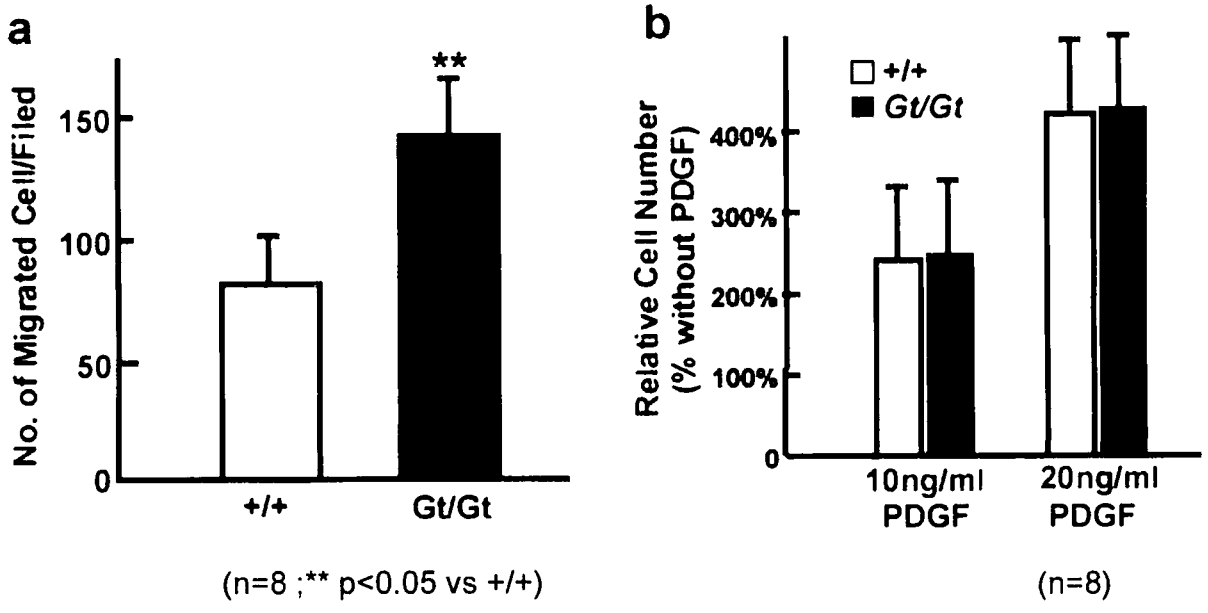

(n=8 ;** p<0.05 vs +/+)

(n=8)

Figure. 14 Cuff Placement Method

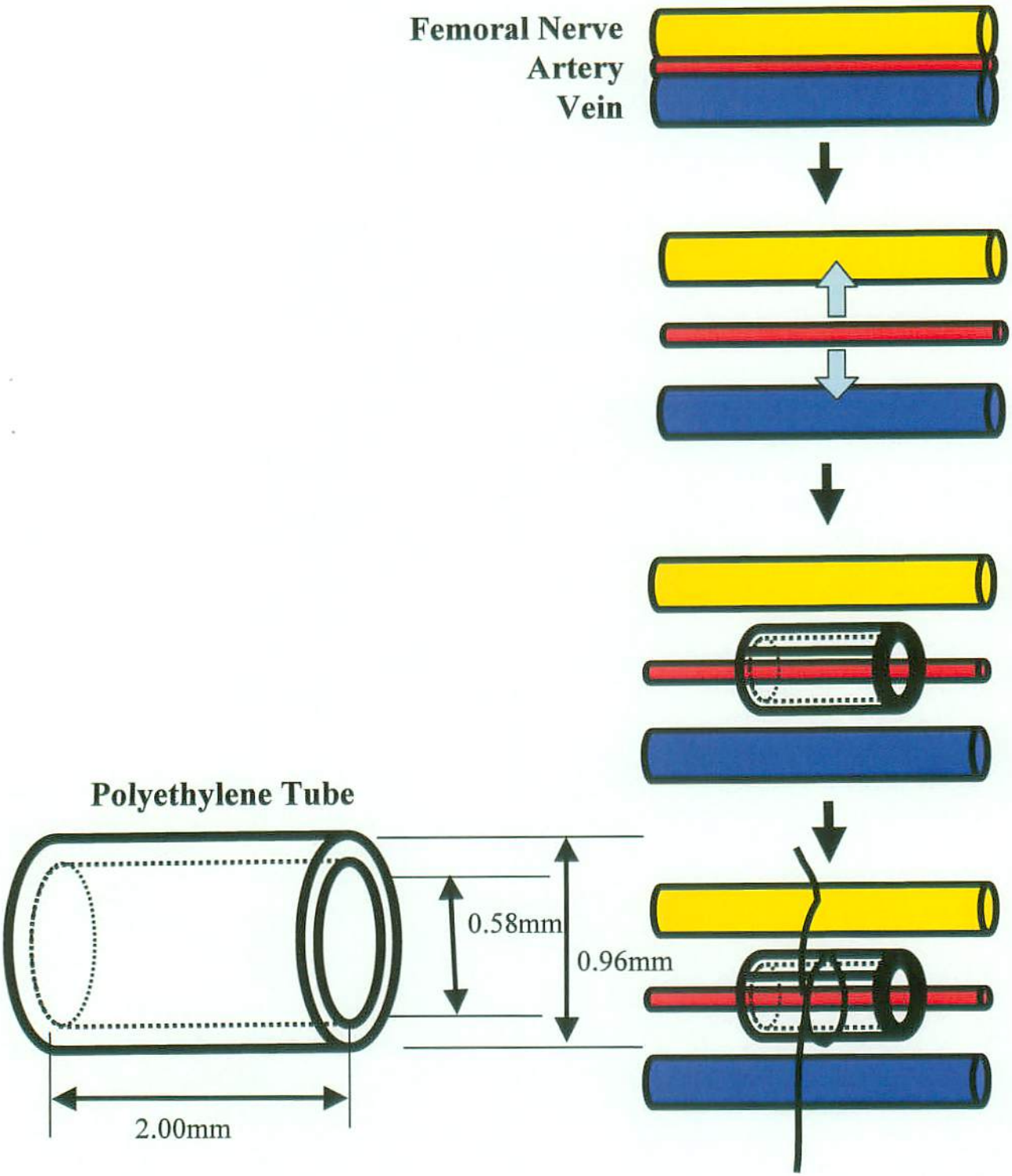

Figure. 15 Cuff Placement 21 Days After Operation

a

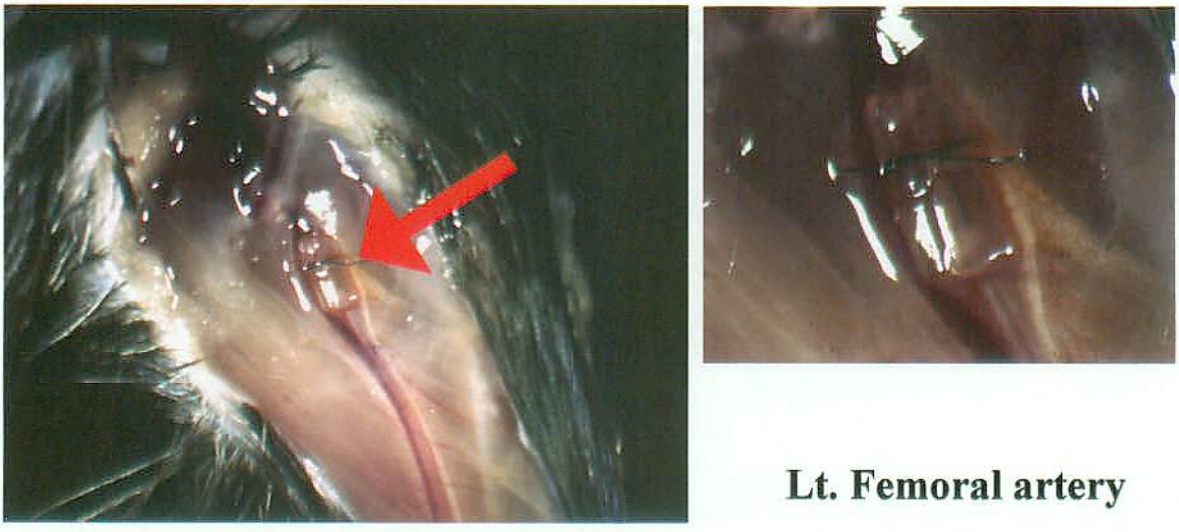

Lt. Femoral artery

b

Figure. 16 Function of *Abhd2 in vivo*

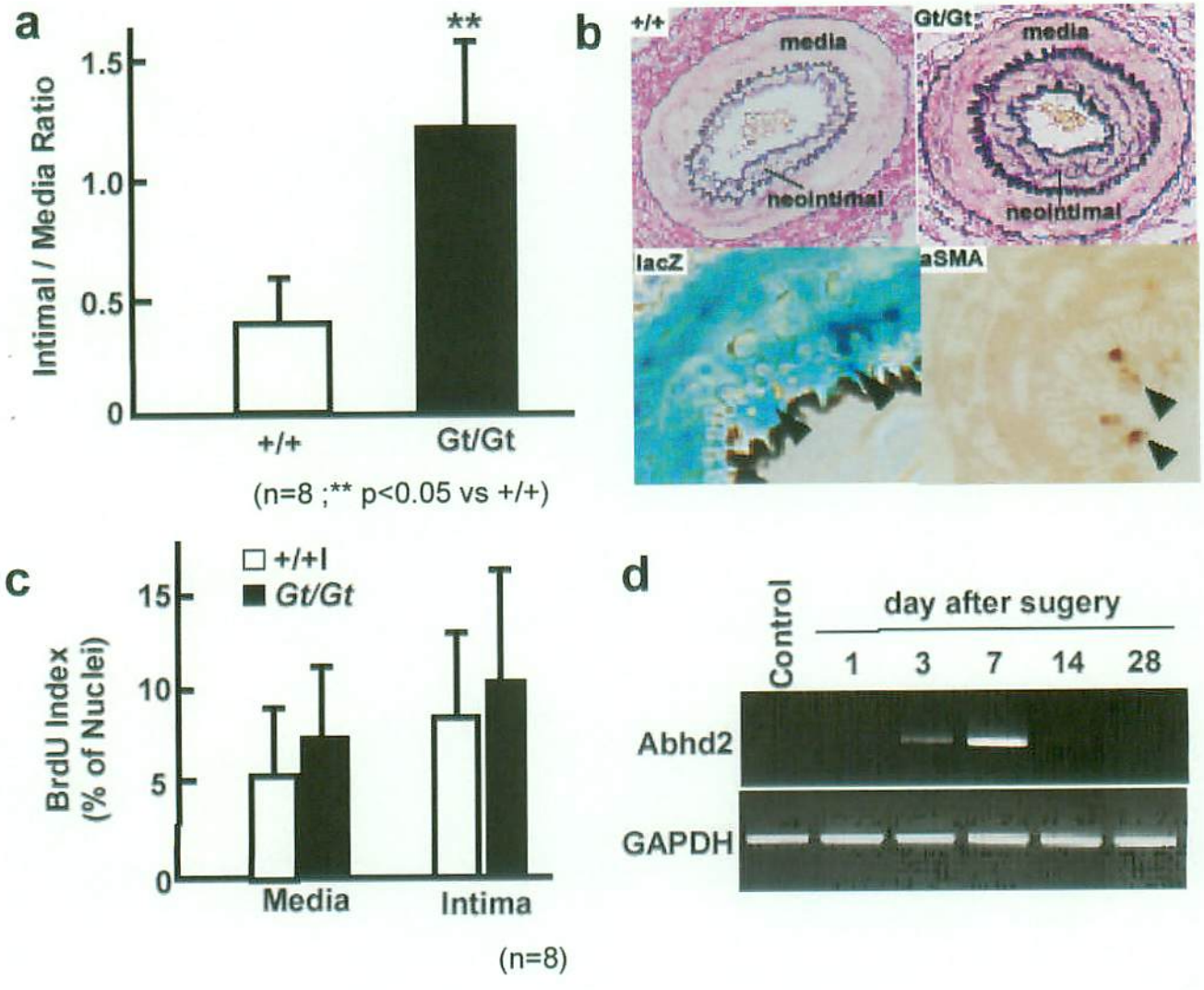

Figure. 17

Murine Abhd2 and Human ABHD2 Homology

Protein Similarity 98.59% /425aa (from NCBI)

References

Araki, K., T. Imaizumi, K. Okuyama, Y. Oike and K. Yamamura (1997). "Efficiency of recombination by Cre transient expression in embryonic stem cells: comparison of various promoters." J Biochem (Tokyo) **122**(5): 977-82

Araki, K., T. Imaizumi, T. Sekimoto, K. Yoshinobu, J. Yoshimuta, M. Akizuki, K. Miura, M. Araki and K. Yamamura (1999). "Exchangeable gene trap using the Cre/mutated lox system." Cell Mol Biol (Noisy-le-grand) **45**(5): 737-50

Athenstaedt, K., D. Zweytick, A. Jandrositz, S. D. Kohlwein and G. Daum (1999). "Identification and characterization of major lipid particle proteins of the yeast Saccharomyces cerevisiae." J Bacteriol **181**(20): 6441-8

Axel, D. I., A. Frigge, J. Dittmann, H. Runge, I. Spyridopoulos, R. Riessen, R. Viebahn and K. R. Karsch (2001). "All-trans retinoic acid regulates proliferation, migration, differentiation, and extracellular matrix turnover of human arterial smooth muscle cells." Cardiovasc Res **49**(4): 851-62

Bellugi, U., L. Lichtenberger, D. Mills, A. Galaburda and J. R. Korenberg (1999). "Bridging cognition, the brain and molecular genetics: evidence from Williams syndrome." Trends Neurosci **22**(5): 197-207

Bonaldo, P., K. Chowdhury, A. Stoykova, M. Torres and P. Gruss (1998). "Efficient gene trap screening for novel developmental genes using IRES beta geo vector and in vitro preselection." Exp Cell Res **244**(1): 125-36

Booth, R. F., J. F. Martin, A. C. Honey, D. G. Hassall, J. E. Beesley and S. Moncada (1989). "Rapid development of atherosclerotic lesions in the rabbit carotid artery induced by perivascular manipulation." Atherosclerosis **76**(2-3): 257-68

Chacos, N., J. Capdevila, J. R. Falck, S. Manna, C. Martin-Wixtrom, S. S. Gill, B. D. Hammock and R. W. Estabrook (1983). "The reaction of arachidonic acid epoxides (epoxyeicosatrienoic acids) with a cytosolic epoxide hydrolase." Arch Biochem Biophys **223**(2): 639-48

Chanarin, I., D. Samson, A. Lang, R. Casey, P. A. Lorkin and H. Lehmann (1975). "Erythraemia due to haemoglobin San Diego." Br J Haematol **30**(2): 167-75

Chen, J., J. W. Streb, K. M. Maltby, C. M. Kitchen and J. M. Miano (2001). "Cloning of a novel retinoid-inducible serine carboxypeptidase from vascular smooth muscle cells." J Biol Chem **276**(36): 34175-81

Chowdhury, K., P. Bonaldo, M. Torres, A. Stoykova and P. Gruss (1997). "Evidence for the stochastic integration of gene trap vectors into the mouse germline." Nucleic Acids Res **25**(8): 1531-6

Clowes, A. W., J. L. Breslow and M. J. Karnovsky (1977). "Regression of myointimal thickening following carotid endothelial injury and development of aortic foam cell lesions in long term hypercholesterolemic rats." Lab Invest **36**(1): 73-81

Couffinhal, T., M. Silver, L. P. Zheng, M. Kearney, B. Witzenbichler and J. M. Isner (1998). "Mouse model of angiogenesis." Am J Pathol **152**(6): 1667-79

Davis, B. B., D. A. Thompson, L. L. Howard, C. Morisseau, B. D. Hammock and R. H. Weiss (2002). "Inhibitors of soluble epoxide hydrolase attenuate vascular smooth muscle cell proliferation." Proc Natl Acad Sci U S A **99**(4): 2222-7

Dorfman, M. L., C. Hershko, S. Eisenberg and F. Sagher (1974). "Ichthyosiform dermatosis with systemic lipidosis." Arch Dermatol **110**(2): 261-6

Edgar, A. J. and J. M. Polak (2002). "Cloning and tissue distribution of three murine alpha/beta hydrolase fold protein cDNAs." Biochem Biophys Res Commun **292**(3): 617-25

Evans, M. J., M. B. Carlton and A. P. Russ (1997). "Gene trapping and functional genomics." Trends Genet **13**(9): 370-4

Fang, X., T. L. Kaduce, N. L. Weintraub, M. VanRollins and A. A. Spector (1996). "Functional implications of a newly characterized pathway of 11,12-epoxyeicosatrienoic acid metabolism in arterial smooth muscle." Circ Res **79**(4): 784-93

Fornage, M., E. Boerwinkle, P. A. Doris, D. Jacobs, K. Liu and N. D. Wong (2004). "Polymorphism of the soluble epoxide hydrolase is associated with coronary artery calcification in African-American subjects: The Coronary Artery Risk Development in Young Adults (CARDIA) study." Circulation **109**(3): 335-9

Gossler, A., A. L. Joyner, J. Rossant and W. C. Skarnes (1989). "Mouse embryonic stem cells and reporter constructs to detect developmentally regulated genes." Science **244**(4903): 463-5

Hicks, G. G., E. G. Shi, X. M. Li, C. H. Li, M. Pawlak and H. E. Ruley (1997). "Functional genomics in mice by tagged sequence mutagenesis." Nat Genet **16**(4): 338-44

Holmquist, M. (2000). "Alpha/Beta-hydrolase fold enzymes: structures, functions and mechanisms." Curr Protein Pept Sci **1**(2): 209-35

Hotelier, T., L. Renault, X. Cousin, V. Negre, P. Marchot and A. Chatonnet (2004). "ESTHER, the database of the alpha/beta-hydrolase fold superfamily of proteins." Nucleic Acids Res **32 Database issue**: D145-7

Imai, Y., T. Shindo, K. Maemura, M. Sata, Y. Saito, Y. Kurihara, M. Akishita, J. Osuga, S. Ishibashi, K. Tobe, H. Morita, Y. Oh-hashi, T. Suzuki, H. Maekawa, K. Kangawa, N. Minamino, Y. Yazaki, R. Nagai and H. Kurihara (2002). "Resistance to neointimal hyperplasia and fatty streak formation in mice with adrenomedullin overexpression." Arterioscler Thromb Vasc Biol **22**(8): 1310-5

Ip, J. H., V. Fuster, L. Badimon, J. Badimon, M. B. Taubman and J. H. Chesebro (1990). "Syndromes of accelerated atherosclerosis: role of vascular injury and smooth muscle cell proliferation." J Am Coll Cardiol **15**(7): 1667-87

Kawazoe, Y., T. Sekimoto, M. Araki, K. Takagi, K. Araki and K. Yamamura (2002). "Region-specific gastrointestinal Hox code during murine embryonal gut development." Dev Growth Differ **44**(1): 77-84

Kietzmann, T. and K. Jungermann (1997). "Modulation by oxygen of zonal gene expression in liver studied in primary rat hepatocyte cultures." Cell Biol Toxicol **13**(4-5): 243-55

Kockx, M. M., G. R. De Meyer, L. J. Andries, H. Bult, W. A. Jacob and A. G. Herman (1993). "The endothelium during cuff-induced neointima formation in the rabbit carotid artery." Arterioscler Thromb **13**(12): 1874-84

Kuzuya, M. and A. Iguchi (2003). "Role of matrix metalloproteinases in vascular remodeling." J Atheroscler Thromb **10**(5): 275-82

Lefevre, C., F. Jobard, F. Caux, B. Bouadjar, A. Karaduman, R. Heilig, H. Lakhdar, A. Wollenberg, J. L. Verret, J. Weissenbach, M. Ozguc, M. Lathrop, J. F. Prud'homme and J. Fischer (2001). "Mutations in CGI-58, the gene encoding a new protein of the esterase/lipase/thioesterase subfamily, in Chanarin-Dorfman syndrome." Am J Hum Genet **69**(5): 1002-12

Levine, G. N., A. P. Chodos and J. Loscalzo (1995). "Restenosis following coronary angioplasty: clinical presentations and therapeutic options." Clin Cardiol **18**(12): 693-703

Lindner, V., J. Fingerle and M. A. Reidy (1993). "Mouse model of arterial injury." Circ Res **73**(5): 792-6

Malinow, M. R., P. B. Duell, D. L. Hess, P. H. Anderson, W. D. Kruger, B. E. Phillipson, R. A. Gluckman, P. C. Block and B. M. Upson (1998). "Reduction of plasma homocyst(e)ine levels by breakfast cereal fortified with folic acid in patients with coronary heart disease." N Engl J Med **338**(15): 1009-15

Merla, G., C. Ucla, M. Guipponi and A. Reymond (2002). "Identification of additional transcripts in the Williams-Beuren syndrome critical region." Hum Genet **110**(5): 429-38

Moroi, M., L. Zhang, T. Yasuda, R. Virmani, H. K. Gold, M. C. Fishman and P. L. Huang (1998). "Interaction of genetic deficiency of endothelial nitric oxide, gender, and pregnancy in vascular response to injury in mice." J Clin Invest **101**(6): 1225-32

Morris, C. A., S. A. Demsey, C. O. Leonard, C. Dilts and B. L. Blackburn (1988). "Natural history of Williams syndrome: physical characteristics." J Pediatr **113**(2): 318-26

Mountford, P., B. Zevnik, A. Duwel, J. Nichols, M. Li, C. Dani, M. Robertson, I. Chambers and A. Smith (1994). "Dicistronic targeting constructs: reporters and modifiers of mammalian gene expression." Proc Natl Acad Sci U S A **91**(10): 4303-7

Nagano, H., R. N. Mitchell, M. K. Taylor, S. Hasegawa, N. L. Tilney and P. Libby (1997). "Interferon-gamma deficiency prevents coronary arteriosclerosis but not myocardial rejection in transplanted mouse hearts." J Clin Invest **100**(3): 550-7

Newby, A. C. and A. B. Zaltsman (2000). "Molecular mechanisms in intimal hyperplasia." J Pathol **190**(3): 300-9

Nishimoto, S., J. Tawara, H. Toyoda, K. Kitamura and T. Komurasaki (2003). "A novel homocysteine-responsive gene, smap8, modulates mitogenesis in rat vascular smooth muscle cells." Eur J Biochem **270**(11): 2521-31

Niwa, H., K. Araki, S. Kimura, S. Taniguchi, S. Wakasugi and K. Yamamura (1993). "An efficient gene-trap method using poly A trap vectors and characterization of gene-trap events." J Biochem (Tokyo) **113**(3): 343-9

Oike, Y., N. Takakura, A. Hata, T. Kaname, M. Akizuki, Y. Yamaguchi, H. Yasue, K. Araki, K. Yamamura and T. Suda (1999). "Mice homozygous for a truncated form of CREB-binding protein exhibit defects in hematopoiesis and vasculo-angiogenesis." Blood **93**(9): 2771-9

Ollis, D. L., E. Cheah, M. Cygler, B. Dijkstra, F. Frolow, S. M. Franken, M. Harel, S. J. Remington, I. Silman, J. Schrag and et al. (1992). "The alpha/beta hydrolase fold." Protein Eng **5**(3): 197-211

Papakonstantinou, E., G. Karakiulakis, M. Roth and L. H. Block (1995). "Platelet-derived growth factor stimulates the secretion of hyaluronic acid by proliferating human vascular smooth muscle cells." Proc Natl Acad Sci U S A **92**(21): 9881-5

Papakonstantinou, E., M. Roth, L. H. Block, V. Mirtsou-Fidani, P. Argiriadis and G. Karakiulakis (1998). "The differential distribution of hyaluronic acid in the layers of human atheromatic aortas is associated with vascular smooth muscle cell proliferation and migration." Atherosclerosis **138**(1): 79-89

Plump, A. S., J. D. Smith, T. Hayek, K. Aalto-Setala, A. Walsh, J. G. Verstuyft, E. M. Rubin and J. L. Breslow (1992). "Severe hypercholesterolemia and atherosclerosis in apolipoprotein E-deficient mice created by homologous recombination in ES cells." Cell **71**(2): 343-53

Rapiejko, P. J., S. T. George and C. C. Malbon (1988). "Primary structure of a human protein which bears structural similarities to members of the rhodopsin/beta-adrenergic receptor family." Nucleic Acids Res **16**(17): 8721

Rosolowsky, M. and W. B. Campbell (1996). "Synthesis of hydroxyeicosatetraenoic (HETEs) and epoxyeicosatrienoic acids (EETs) by cultured bovine coronary artery endothelial cells." Biochim Biophys Acta **1299**(2): 267-77

Rozenszajn, L., A. Klajman, D. Yaffe and P. Efrati (1966). "Jordans' anomaly in white blood cells. Report of case." Blood **28**(2): 258-65

Savani, R. C., C. Wang, B. Yang, S. Zhang, M. G. Kinsella, T. N. Wight, R. Stern, D. M. Nance and E. A. Turley (1995). "Migration of bovine aortic smooth muscle cells after wounding injury. The role of hyaluronan and RHAMM." J Clin Invest **95**(3): 1158-68

Schrag, J. D. and M. Cygler (1997). "Lipases and alpha/beta hydrolase fold." Methods Enzymol **284**: 85-107

Schwartz, S. M., D. deBlois and E. R. O'Brien (1995). "The intima. Soil for atherosclerosis and restenosis." Circ Res **77**(3): 445-65

Smith, C. A. and D. J. Harrison (1997). "Association between polymorphism in gene for microsomal epoxide hydrolase and susceptibility to emphysema." Lancet **350**(9078): 630-3

Stary, H. C., A. B. Chandler, S. Glagov, J. R. Guyton, W. Insull, Jr., M. E. Rosenfeld, S. A. Schaffer, C. J. Schwartz, W. D. Wagner and R. W. Wissler (1994). "A definition of initial, fatty streak, and intermediate lesions of atherosclerosis. A report from the Committee on Vascular Lesions of the Council on Arteriosclerosis, American Heart Association." Circulation **89**(5): 2462-78

Sulkowska, M., S. Sulkowski and J. Dzieciol (1996). "Type II alveolar epithelial cells promote fibrosis during development of experimental lung emphysema." Folia Histochem Cytobiol **34 Suppl 1**: 27-8

Takeyabu, K., E. Yamaguchi, I. Suzuki, M. Nishimura, N. Hizawa and Y. Kamakami (2000). "Gene polymorphism for microsomal epoxide hydrolase and susceptibility to emphysema in a Japanese population." Eur Respir J **15**(5): 891-4

Tanaka, K., M. Sata, Y. Hirata and R. Nagai (2003). "Diverse contribution of bone marrow cells to neointimal hyperplasia after mechanical vascular injuries." Circ Res **93**(8): 783-90

Thurman, R. G. and F. C. Kauffman (1985). "Sublobular compartmentation of pharmacologic events (SCOPE): metabolic fluxes in periportal and pericentral regions of the liver lobule." Hepatology **5**(1): 144-51

Xu, Y., H. Arai, X. Zhuge, H. Sano, T. Murayama, M. Yoshimoto, T. Heike, T. Nakahata, S. Nishikawa, T. Kita and M. Yokode (2004). "Role of bone marrow-derived progenitor cells in cuff-induced vascular injury in mice." Arterioscler Thromb Vasc Biol **24**(3): 477-82

Yagi, T., T. Tokunaga, Y. Furuta, S. Nada, M. Yoshida, T. Tsukada, Y. Saga, N. Takeda, Y. Ikawa and S. Aizawa (1993). "A novel ES cell line, TT2, with high germline-differentiating potency." Anal Biochem **214**(1): 70-6

Yamaguchi, T., N. Omatsu, S. Matsushita and T. Osumi (2004). "CGI-58 interacts with perilipin and is localized to lipid droplets. Possible involvement of CGI-58 mislocalization in Chanarin-Dorfman syndrome." J Biol Chem **279**(29): 30490-7

Yamauchi, Y., K. Abe, A. Mantani, Y. Hitoshi, M. Suzuki, F. Osuzu, S. Kuratani and K. Yamamura (1999). "A novel transgenic technique that allows specific marking of the neural crest cell lineage in mice." Dev Biol **212**(1): 191-203

Zalewski, A. and Y. Shi (1997). "Vascular myofibroblasts. Lessons from coronary repair and remodeling." Arterioscler Thromb Vasc Biol **17**(3): 417-22